



OPEN

Origin of sandy substrates controlling the distribution of open vegetation ecosystems in Amazonia

Fernanda C. G. Rodrigues^{1,5}✉, Camila C. Ribas², Fabiano N. Pupim³, Naomi Porat⁴, Thomas K. Akabane⁵, Alberto Vicentini² & André O. Sawakuchi⁵

Understanding the role of open vegetation, particularly in white-sand ecosystems (WSE) and savannas, is crucial for elucidating their role in Amazonian biotic diversification. These ecosystems predominantly develop on sandy terrains, suggesting that the geological substrate significantly influences the vegetation upon it. Therefore, the interaction between landscape changes and biotic diversification is closely tied to the dynamics and resilience of these sandy substrates. Current WSE and savannas in lowland Amazonia colonized fluvial sediments deposited during the past 120 ka, with marked synchronicity over the last 23 ka, as shown by optically stimulated luminescence (OSL) and radiocarbon ages of such sandy substrates. In contrast, sandy substrates supporting open vegetation in highland areas, unsuitable for Quaternary sand accumulation, would have persisted beyond the Quaternary, as ancient sedimentary rocks in these areas are prone to developing sandy soils. The current distribution of open vegetation ecosystems in lowland Amazonia is coupled with the deposition and erosion of sandy sediments by Quaternary fluvial systems, while weathering sandy substrates in highland areas serve as long-term and resilient refugia beyond the Quaternary. The contrasting spatiotemporal dynamics of landscape changes in lowland and highland areas has implications for biodiversification or extinction events leading to current biogeography patterns in Amazonia.

Beyond its closed canopy megadiverse rainforest, Amazonia holds widespread patches of open vegetation, mainly represented by white-sand ecosystems (WSE) and savannas^{1,2} (Fig. 1). The occurrence and extent of savannas during Pleistocene glacial-interglacial cycles (~100 ka) have occupied the core of the debate about drivers of biotic diversification in Amazonia through the refugia hypothesis, which states that savannas expanded across Amazonia during presumably drier glacial periods, promoting the fragmentation of rainforests and creating conditions for vicariant speciation of forest adapted organisms³. However, paleovegetation records show that most of lowland Amazonia remained covered by forests even during drier and/or cooler periods of the Pleistocene^{4–8}, despite potential changes in the forest structure^{9,10} and a contraction in its southern^{11,12} and southeastern^{13–16} boundaries. Moreover, the pre-Pleistocene origin of most extant plant species points to the importance of processes beyond those related to glacial-interglacial cycles in creating forest diversity¹⁷. Nevertheless, the debate about how the distribution of rainforest and open vegetation ecosystems varied during Pleistocene glacial-interglacial cycles continues^{18–20}, with the spatiotemporal dynamics of open vegetation ecosystems representing a key issue on this debate.

Ecosystems of lowland Amazonia, here considered as the areas up to 200 m elevation, include upland and seasonally flooded forests, WSE and savannas developed upon ancient fluvial^{26–30} and/or alluvial^{31,32} deposits and even over eolian deposits³³. The sedimentary dynamics of fluvial systems changes the distribution and connectivity of upland and seasonally flooded habitats in Amazonia³⁴, influencing biotic patterns in several ways. In a million-year timescale, large rivers represent major biogeographic boundaries for upland species³⁵. In a thousand-year timescale, phases of channel incision promoted the fragmentation of floodplains and restricted gene flow of birds adapted to seasonally flooded vegetation³⁶. WSE are mainly distributed over abandoned fluvial deposits along sectors of the Negro, Branco and Madeira rivers (Fig. 1). Thus, fluvial systems could also influence WSE biodiversity. WSE plant and bird communities are highly endemic and distinct from other Amazonian

¹School of Arts, Sciences and Humanities, University of São Paulo, São Paulo, SP, Brazil. ²National Institute of Amazonian Research, Manaus, AM, Brazil. ³Department of Environmental Sciences, Federal University of São Paulo, Diadema, SP, Brazil. ⁴Geological Survey of Israel, Jerusalem, Israel. ⁵Institute of Geosciences, University of São Paulo, São Paulo, SP, Brazil. ✉email: cgrfernanda@usp.br

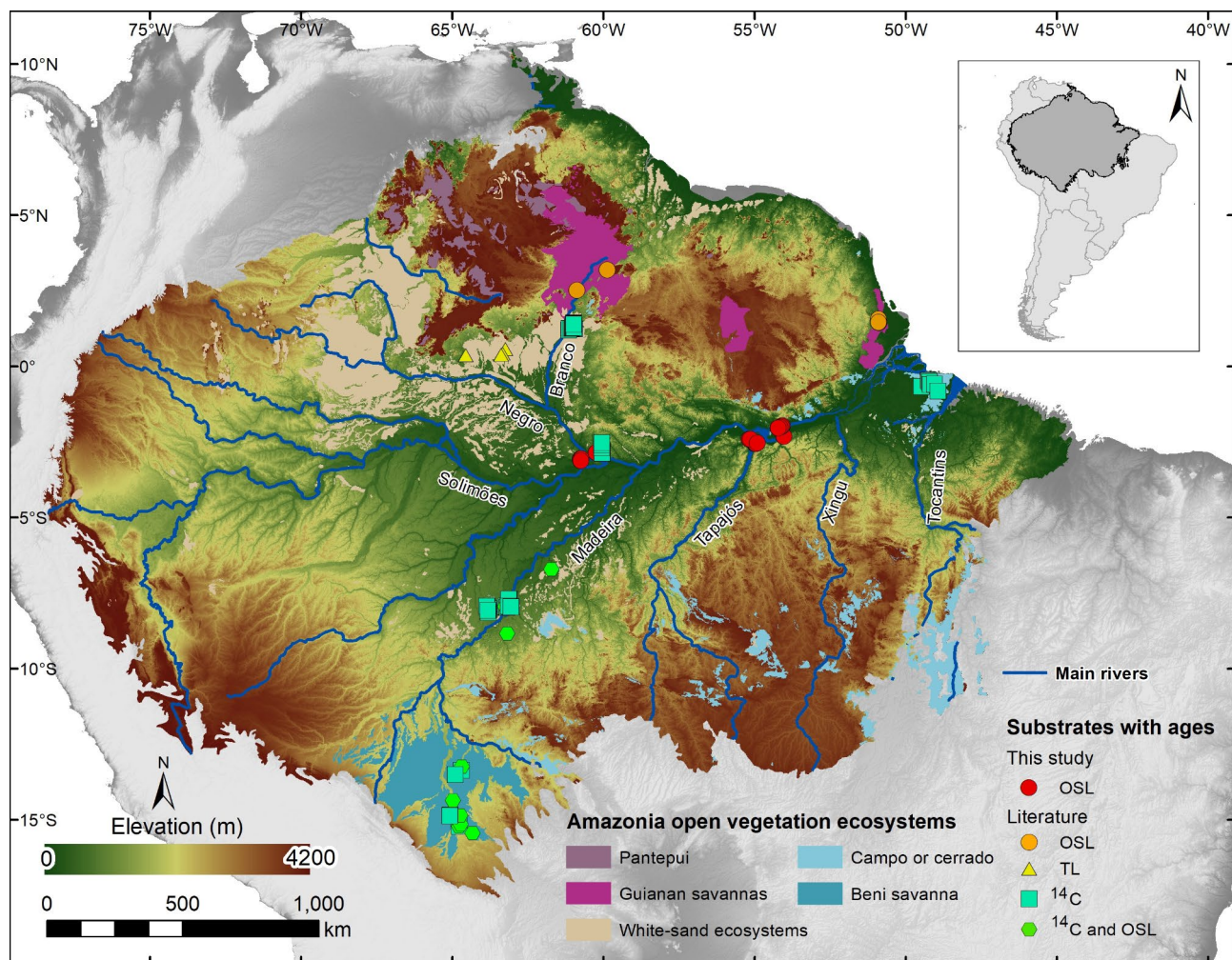


Fig. 1. Distribution of open vegetation ecosystems within the Amazonia biome and sites with OSL and radiocarbon (^{14}C) ages for the substrates supporting these ecosystems. The inset on the top right shows the Amazonia biome within the South America continent. Sites sampled in this study can be observed in more detail in Figs. 3, 4 and 5. Geographical coordinates of samples and ages data are shown in Supplementary Tables S1 and S2. This map was created with ArcMap 10.8 software (<https://www.esri.com/en-us/arcgis/products/arcgis-desktop/resources>). Data sources: South America boundaries - U.S. Department of State, Office of the Geographer. (2013); digital elevation data - USGS EROS Archive Shuttle Radar Topography Mission (SRTM) Void Filled resampled to 1 km resolution; rivers - ESRI and CPRM (<https://geosgb.sgb.gov.br/>); Amazon boundary, Beni savanna and Pantepui - Olson et al.²¹, Guianan savannas and Campos or cerrado - courtesy of Alberto Vicentini and INPA GIS Lab, M. Alencar and A. Carneiro; White-sand ecosystems - IBGE hydromorphic spodosols (<https://www.ibge.gov.br/geociencias/informacoes-ambientais/pedologia/10871-pedologia.html?=&t=downloads>), files courtesy of Alberto Vicentini and INPA GIS Lab, M. Alencar and A. Carneiro, including files based on Radambrasil²², ter Steege and Zondervan²³, Vriesendorp et al.²⁴ and Josse et al.²⁵, and files courtesy of H. ter Steege for Colombia and Suriname WSE.

environment's biota, including the savanna biota^{1,2,37}. This suggests a persistent availability of fragmented WSE areas suitable to support the evolution of specialized biota. The Amazonian savanna ecosystems mostly occur in southwestern Amazonia in Bolivia and in eastern and northern Amazonia in Brazil³⁸, and share many plant and animal species with the Brazilian *cerrado*³⁹, fueling the discussion of past connections between these biomes and the expansion of the 'dry corridor' in Amazonia²⁰. Savannas in eastern and northern Amazonia occur mostly on fluvially deposited sandy substrates, which can also host the adjacent rainforest⁴⁰. The biota associated with Amazonian savannas have lower endemism compared to the rainforest and WSE^{37,41}, pointing to greater biological connectivity with surrounding non-Amazonian savannas through time and/or higher rates of extinction due to conversion into closed forest.

Amazonian WSE and savannas occur mostly over sandy substrates formed by either fluvial sediment deposition (or locally by eolian deposition supplied by rivers) during the Neogene and Quaternary^{33,42,43} or due to in situ weathering of parent rocks with varied formation ages^{44–46}. Thus, figuring out the spatiotemporal

dynamics and the resilience of sandy substrates is essential to shed light on the interaction between physical landscape changes and biotic diversification⁴⁷.

This study aims to understand the factors controlling the development of sandy substrates sustaining WSE and savannas in Amazonia. We focus on two main research questions: (1) What are the formation ages of the sandy substrates supporting WSE and savannas? (2) How do these ages and the sand origins aid in our understanding of Amazonian biogeography? To answer these questions, we used optically stimulated luminescence (OSL) and radiocarbon dating to determine the ages of sandy substrates in central and eastern Amazonia, combined with extensive OSL and radiocarbon ages compiled from the literature. Additionally, we analyzed the OSL sensitivity of quartz sand grains to differentiate between sediments from cratonic and Andean rivers⁴⁸. This approach helps us infer the geological history of these sandy substrates. Our findings provide insights into the interaction between landscape changes and biotic diversification, shedding light on the processes shaping Amazonian biodiversity patterns.

Background on types and origins of the Amazonian open vegetation substrates

Amazonian open vegetation ecosystems include: (i) the Pantepui on the summits of table mountains in northern Amazonia, (ii) savannas on the upland plains of the Guiana Shield and as enclaves on the lowlands in eastern and southern Amazonia, (iii) white-sand grasslands, shrublands and forests occurring mainly on the Negro and Madeira rivers basins, respectively in the northwestern and southwestern lowland Amazonia, (iv) the Beni savannas in the Madeira River basin in southwestern Amazonia, and (v) several patches of *campo* or *cerrado* vegetation from southwestern to northeastern Amazonia and at the borders of the biome (Table 1; Fig. 1).

The Pantepui occurs on the summits of the Guiana Shield, at elevations from 1100 m to 3000 m⁵⁶, associated with waterlogged soils developed upon weathered and bare Paleoproterozoic (~1.8 Ga) quartzites and sandstones of the Roraima Supergroup^{57–59}. The Pantepui vegetation is strongly linked ecologically and phylogenetically to the lowland WSE⁶⁰. Ruprestrial savannas, called *cerrado* or *campo rupestre*, also occur on shallow soils developed upon similar Paleoproterozoic quartzites and sandstones of the Central Brazil Shield^{61,62} in southeastern Amazonia.

WSE occur as patches of open herbaceous areas, woodlands, scrublands and low-stature forests developed upon sandy substrates, embedded into the upland *terra-firme* rainforest and/or mixed with savanna ecosystems^{1,49,63}. WSE are usually associated with leached quartz-rich sandy substrates and host endemic biota, whose evolutionary origin and temporal variations are still poorly constrained^{2,64}. White-sand substrates in northeastern Peru are linked to fluvial deposits and are composed almost solely of quartz sand grains and were likely deposited by an eastward fluvial system draining the craton^{65,66}. The WSE from the Negro and Branco rivers basins in northern Amazonia occur upon deposits of large distributary fluvial systems, known as megafans (e.g., Viruá megafan). These substrates are composed of fine to medium quartzose sands sourced in the Precambrian rocks of the Guiana Shield and were deposited from 38 ka up to mid-Holocene⁶⁷. In this same region, eolian sands deposited by NE winds between 32 and 8 ka also sustain WSE⁶⁸. WSE occur typically associated with hydromorphic spodosols, especially in the Negro River basin¹. In Amazonia, spodosols are described as formed upon Quaternary fluvial sediments deposited on the edge of incised fluvial valleys⁶⁹, on fluvial terraces⁷⁰, on weathered sandstones of the Late Cretaceous Alter do Chão Formation⁴⁴, on the sands and sandy clays of the Plio-Pleistocene White Sands (or Berbice) Formation^{71,72} and on previously formed oxisols^{45,73,74}. These current spodosols have been under development in central Amazonia at least during the Holocene, as indicated by radiocarbon ages of 3 to 2 ka obtained in organic sediments of black wavy bands in the E horizon⁴⁴. Some WSE and savanna substrates are also derived from weathering and leaching of sandy substrates, without the formation of spodosols, as the weathering of quartzites of the Guiana Shield (Roraima Supergroup) and Paleozoic sandstones of the Amazonas sedimentary basin^{44,75,76}.

The Amazonian savanna ecosystems encompass grasslands and open woodlands in isolated patches, mostly occurring in southwestern Amazonia in Bolivia (Beni savannas) and in eastern and northern Amazonia in Brazil (Guianan savannas) (De Carvalho and Mustin, 2017) (Fig. 1). Guianan savannas occur mainly upon Quaternary eolian and fluvial deposits laid upon incipient or evolved lateritic soils⁷⁷. Eolian deposits with well-preserved dune features were formed by NE blowing winds during drier phases of the Late Pleistocene and Holocene (OSL ages ranging from 23 to 1 ka)^{33,78}, whilst fluvial and alluvial sand and silt deposits occur both laterally and overlain by the eolian deposits, with ages ranging from 52 to 28 ka³³. In the middle Madeira River in Southwestern Amazonia, savanna patches develop upon fluvial channel sandy sediments, deposited between 119 and 36 ka⁴³. These sandy deposits are locally overlain by muddy successions from abandoned channels and

Ecosystem	Description
Pantepui	Broadleaved meadows, scrubs, woodland and low forests occurring on the <i>tepui</i> (tabletop mountains) of the Guiana Shield.
White-sand ecosystems (WSE)	Grasslands, shrublands and forests associated with quartz-rich sandy soils occurring mainly in lowland areas. These ecosystems sustain vegetation types known as <i>campinas</i> and/or <i>campinaranas</i> .
Guianan savannas	Tropical mixed tree-grass systems, with a continuous grass layer and a discontinuous tree canopy forming mosaics with varying densities of tree canopy.
Beni savannas	Herbaceous wetlands, grasslands, and woodlands shaped by cycles of drought and flooding.
<i>Campo</i> or <i>cerrado</i>	Grasslands with shrubs and small trees on acidic well-drained soils, including savanna vegetation upon lateritic crusts, locally known as <i>canga</i> vegetation.

Table 1. Description of the Amazonia open vegetation ecosystems discussed in this study^{1,49–55}. Distribution of the ecosystems summarized below is shown on Fig. 1.

floodplain complexes younger than 26 ka⁴³. The Beni savannas occur in the wetlands of southwestern Amazonia, developed upon fluvial and alluvial clayey deposits accumulated by rivers with Andean headwaters^{79,80}, spanning from 19.1 to 1.3 ka^{31,32,81}, according to OSL and radiocarbon ages. These wetlands are formed as a result of rearrangement of the drainage system, due to autogenic processes, tectonic and climate changes, inducing changes in flooding patterns^{31,32}, therefore influencing the forest-savanna boundaries⁸².

Campo or *cerrado* encompasses more savanna-like environments, including the savannas of the Marajó Island in northeastern Amazonia developed upon Pleistocene and Holocene fluvial deposits spanning from 55 to 6 ka, as recorded by radiocarbon dating of peat, wood, plant remains and bulk organic sediments⁸³. This fluvial environment was very dynamic during the Holocene, changing from continental influenced to tidally influenced settings, followed by a lacustrine phase before returning to the current more continental conditions⁸³. Moreover, *campo* also encompasses a particular montane savanna ecosystem, called *canga* vegetation, which develops upon ironstone formation^{50,84}.

The role of climate on shaping Amazonian ecosystems

Climate changes related to Quaternary glacial-interglacial cycles, such as atmospheric CO₂ concentration, temperature, and sea-level fluctuations, mostly followed a 41 or 100 kyr cycle^{85,86}. However, it has been shown that precipitation changes across Amazonia are controlled by shifts of the South American Monsoon System (SAMS) (Fig. 2), which mainly follows precession insolation cycles of ~ 23 ka⁸⁷ punctuated by abrupt millennial events, such as Heinrich Stadials^{6,88}. Despite the recurrence of these combined environmental changes, a predominant forest cover long remained in the Amazon basin but marked by important floristic changes (e.g., Refs.^{4,6,7}). Nevertheless, a significant savanna expansion mostly featured over the surrounding ecotone regions^{11,12,15}. Lower atmospheric CO₂ concentration⁸⁶ and regionally drier conditions⁸⁸ negatively affected forest development, while cooler glacial temperatures may have attenuated these effects⁸.

Lake sediment records from montane savanna ecosystems (also referred as *canga* vegetation) in Serra Sul de Carajás, in southeastern Amazonia, show shifts from wet to dry periods over the last 70 ka, with rainforest expansion during wetter phases^{13,14,16}. In the region of the Beni savannas, the boundaries between savannas and rainforest shifted during the Holocene, with rainforest expansion in the last 3 ka due to a southward shift of the ITCZ^{12,92,93}. However, the persistence of open vegetation in areas with varied precipitation patterns and surrounded by rainforest under the same precipitation patterns (Fig. 2) suggests controls beyond regional climate in Amazonia.

Methods

Field descriptions and sediment sampling

Satellite images available on Google Earth combined with the dataset of distribution of open vegetation ecosystems within the Amazonia biome (available in Adeney et al.¹) were used to identify preserved depositional morphologies and determine the locations for sediment description and sampling for OSL dating, as well as

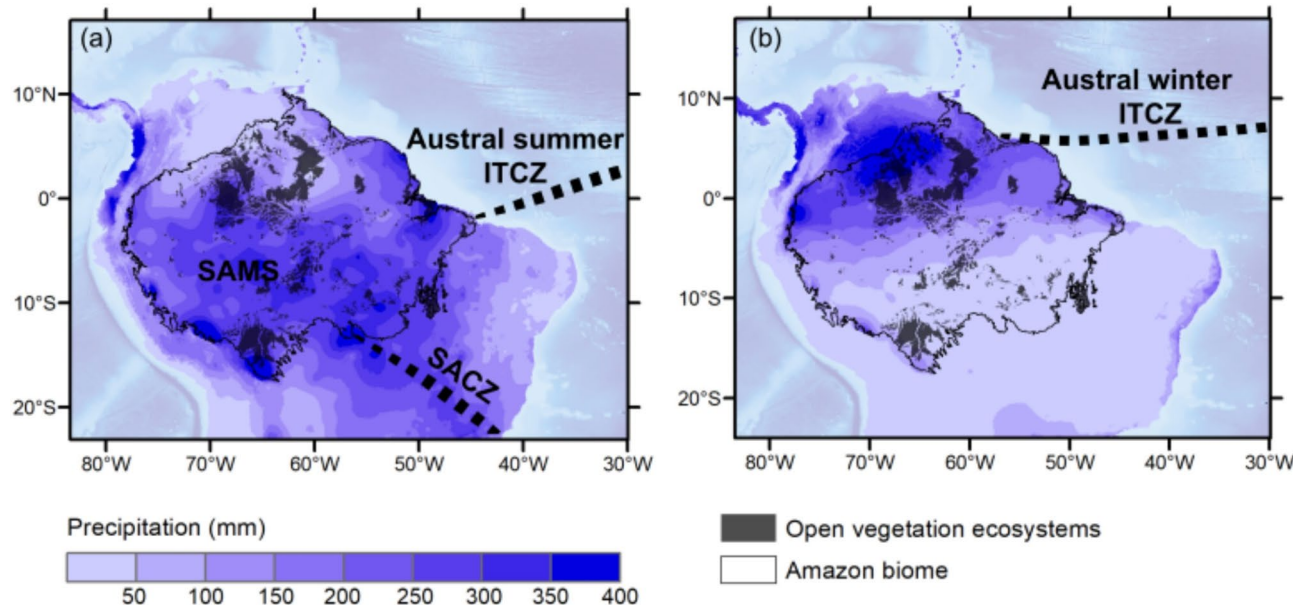


Fig. 2. Monthly averaged terrestrial precipitation (2010–2018) (CRU-TS 4.03⁸⁹ downscaled with WorldClim 2.1⁹⁰) for (a) austral summer (December–January–February (DJF)) and (b) austral winter (June–July–August (JJA)). The schematic positions of the Intertropical Convergence Zone (ITCZ) over the Atlantic during DJF (a) and JJA (b) as well as the South Atlantic Convergence Zone (SACZ) (a) (thick dashed lines) are also shown⁹¹. SAMS: South American monsoon system. This map was created with ArcMap 10.8 software (<https://www.esri.com/en-us/arcgis/products/arcgis-desktop/resources>).

to estimate the areas (km^2) of the open vegetation patches (Fig. 3). The sedimentary deposits were described in outcrops or excavated trenches (up to 2 m depth), according to a sedimentary facies analysis approach. The deposits were described considering their texture (grain size and sorting) and sedimentary structures. Post-depositional weathering features were also considered due to the massive and altered nature of most deposits. Field descriptions and sampling for OSL dating and sensitivity were performed during two fieldworks surveys carried out in July 2018 and August 2019. Graphic sedimentological logs are presented in Figs. 7, 8 and 9.

OSL dating

OSL dating was carried out on single aliquots of quartz in the 180–250 μm fraction. The preparation of quartz concentrates was performed under subdued amber light and consisted of the following steps: (i) separation of 180–250 μm grains through wet sieving; (ii) treatment with H_2O_2 35% and HCl 10% to eliminate organic matter and carbonate minerals, respectively; (iii) density separation with lithium metatungstate (LMT) solutions at densities of 2.62 g/cm^3 and 2.75 g/cm^3 to isolate quartz grains from feldspar and heavy minerals; (iv) treatment with HF 40% to eliminate the outer rind of quartz grains affected by alpha radiation; (v) another sieving of 180–250 μm grains to separate them from quartz with reduced grain sizes after the previous treatment. All luminescence measurements were carried out in Risø TL/OSL readers model DA-20 system, equipped with $^{90}\text{Sr}/^{90}\text{Y}$ beta source (dose rates of 0.12–0.07 Gy/s for stainless steel discs), blue and infrared LEDs for stimulation and 7.7 mm Hoya U-340 filter for light detection in the ultraviolet band.

OSL dating followed the quartz single-aliquot regenerative-dose (SAR) protocol (Table 2, ⁹⁴). The suitability of the OSL-SAR protocol for estimation of equivalent doses (D_e) under laboratory conditions was evaluated by dose recovery tests (Supplementary Table S3). For each sample, 12 to 24 aliquots of 5 mm were measured, and the D_e was calculated using the Central Age Model (CAM) as proposed by Galbraith et al. ⁹⁵ and the Minimum Age Model (MAM) (LDAC, Liang and Forman ⁹⁶). For samples with overdispersion $< 30\%$, we considered the CAM D_e , and for samples with overdispersion $> 30\%$, we considered the MAM D_e . D_e distributions are represented by kernel density plots in Figs. 7, 8 and 9.

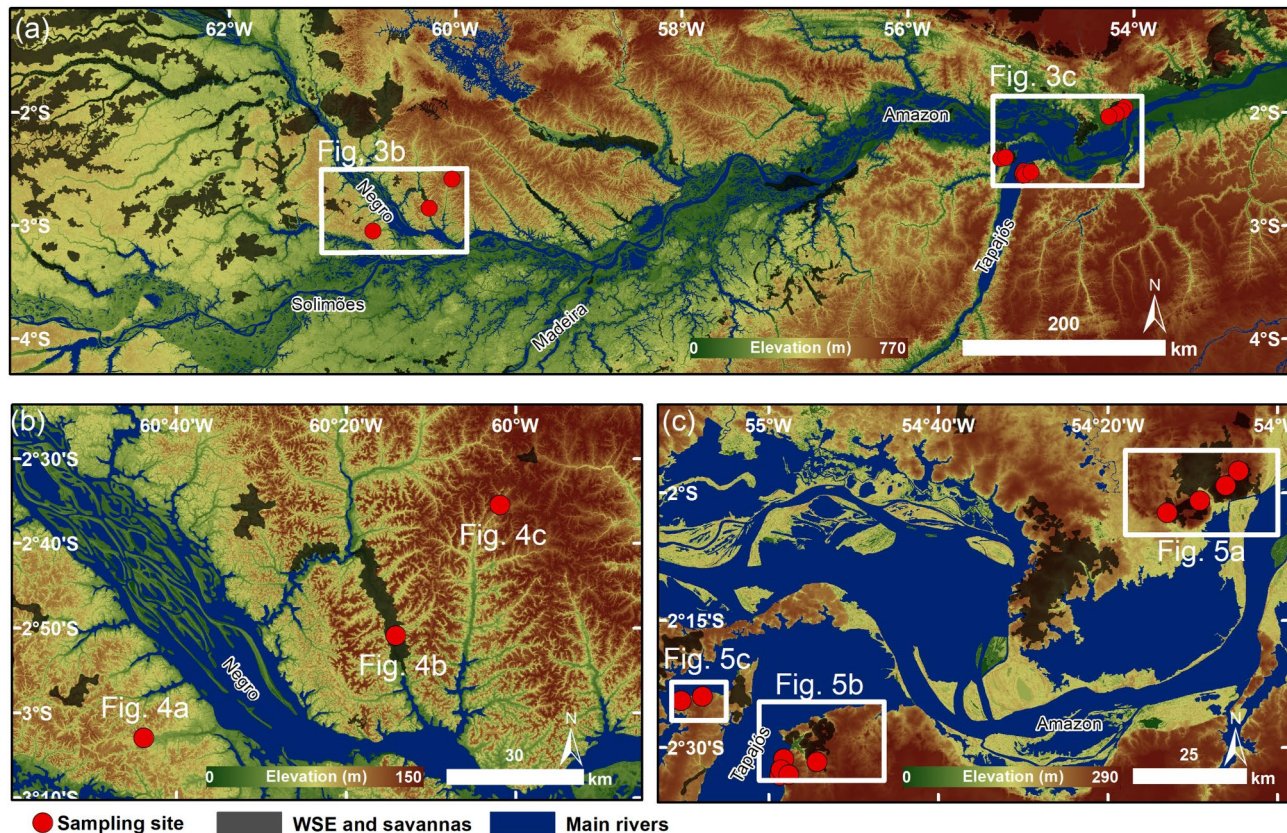


Fig. 3. (a) Sampling sites for OSL dating of sandy substrates of WSE and savannas in central and eastern Amazonia; (b) WSE patches in central Amazonia and sampling sites, (c) savanna patches on eastern Amazonia and sampling sites. This map was created with ArcMap 10.8 software (<https://www.esri.com/en-us/arcgis/products/arcgis-desktop/resources>). Data sources: digital elevation data - USGS EROS Archive Shuttle Radar Topography Mission (SRTM) Void Filled resampled to 250 m resolution; rivers - CPRM (<https://geosgb.sgb.gov.br/>); savannas and WSE - courtesy of Alberto Vicentini and INPA GIS Lab, M. Alencar and A. Carneiro, and IBGE hydromorphic spodosols (<https://www.ibge.gov.br/geociencias/informacoes-ambientais/pedologia/10871-pedologia.html?=&t=downloads>).

Step	OSL – SAR protocol ⁹⁴	Sensitivity protocol ⁴⁸
1	Give dose D_i	Illumination with Blue LED at 25 °C for 100 s
2	Preheat at 200, 220 or 260 °C for 10 s ^a	Give dose, 10 Gy
3	Blue LED stimulation for 40 s at 125 °C	Pre-heat at 190 °C for 10 s
4	Give test dose, D_t	IRSL LED stimulation at 60 °C for 300 s
5	Cutheat at 160 or 220 °C ^a	Blue LED stimulation for 100 s at 125 °C (BOSL)
6	Blue LED stimulation for 40 s at 125 °C	
7	Blue LED stimulation for 40 s at 280 °C ^a	
8	Return to step 1	

Table 2. Quartz single-aliquot regenerative-dose (SAR) protocol⁹⁴ used for dating and sensitivity analysis protocol⁴⁸ used in this study. $D_1 < D_2 < D_3 < D_4$, $D_5 = 0$ Gy, $D_6 = D_1$, $D_7 = D_1$ (with infrared stimulation before blue stimulation)(natural signal, $i = 0$ and D_0 = natural dose). ^aSample dependent, for more information, see Supplementary Material Table S1. Recuperation was calculated through D_5 signal, recycling ratio was calculated through D_6 and D_1 signals and feldspar contamination was appraised through D_6 and D_7 signals.

Radionuclides concentrations for determination of radiation dose rates from sediments were estimated using high resolution gamma spectrometry with a high-purity germanium gamma-ray detector (Canberra Instruments, relative efficiency of 55% and energy resolution of 2.1 keV) encased in an ultralow background shield. Sediment samples were dried for packing in plastic sealed containers and stored for at least 28 days for Rn re-equilibrium before gamma spectrometry. The concentrations of ^{238}U (ppm), ^{232}Th (ppm) and ^{40}K (%) were converted into dose rate (Gy/ka) using the conversion factors proposed by Guérin et al.⁹⁷. Cosmic rays' contribution to the dose rate was calculated according to Prescott and Hutton⁹⁸, considering latitude, longitude, altitude, depth below surface and density of each sample.

Further information on sampling and basic sample information (field code, laboratory code, location, etc.) can be found in Supplementary Information (SI) 1 and Supplementary Table S1, respectively.

Quartz OSL sensitivity

Pure quartz aliquots, in the 180–250 μm grain size fraction, were used to measure OSL sensitivity. Three to five aliquots per sample with a diameter of 4 mm were prepared by mounting grains in a steel disc. Each aliquot was weighted in a precision scale for mass-normalization. The luminescence sensitivity protocol (Table 2) following Sawakuchi et al.⁴⁸. The IRSL stimulation (step 4) was used to bleach any remaining feldspar grains before the measurement of quartz OSL sensitivity (step 5).

OSL sensitivity was calculated using the integral of the first 1 s of light emission minus the last 10 s as background (BOSL_{1s}) with normalization by given dose and aliquot mass (photon cts $\text{Gy}^{-1} \text{mg}^{-1}$) and as a percentage of the initial 1 s of light emission in relation to the total OSL emission (%BOSL_{1s}), with subtraction of the last 10 s as background for both total and 1 s signal.

Average %BOSL_{1s} was compared among the sandy substrate samples and with riverbed samples from Sawakuchi et al.⁴⁸, as all measurements were performed on the same luminescence reader.

Compilation of luminescence and ^{14}C ages from the literature

We conducted a comprehensive compilation of published TL, OSL and ^{14}C ages on substrates of the main open vegetation ecosystems across the lowland Amazon region. The published ages combined with the ages produced in this study allowed determining the timing and accumulation rates of these different substrates. Ages were compiled according to the location, ecosystem, dating method, material and depth in the sedimentary profile (Supplementary Table S2). Conventional ^{14}C ages were compiled and calibrated using the software OxCal 4.4 (reported as cal ka BP) according to SHCal20⁹⁹. The median of the calibrated ^{14}C ages was used for graphing purposes. Coarse grained (very fine to fine sand grain size) quartz OSL ages were used to estimate accumulation rates along each profile.

Results

Sedimentology and geomorphology

The sandy substrates of WSE in the lower Negro River in central Amazonia (Fig. 4) and of savannas around the confluence of Tapajós and Amazon rivers in eastern Amazonia (Fig. 5) occur over Paleozoic and Mesozoic sedimentary rocks and lateritic paleosols, which can be partially covered by Neogene-Quaternary sedimentary deposits¹⁰⁰. The sediment profiles of WSE substrates in the interfluviums of both margins of the lower Negro River occur as isolated patches within a rainforest matrix (Fig. 4). The white-sand patch usually has less than 1 km^2 in area and occurs at elevations from 50 to 100 m. These sediment profiles are composed of massive, loose, poorly sorted, white to grayish coarse sands (Figs. 6a and b and 7). In the profile AVA-23 (Fig. 6b), a thin and poorly developed organic-rich horizon (< 5 cm thick) occurs at the top of the grayish coarse sands. The sandy substrates of the savannas of eastern Amazonia occur as patches with unit areas from 2 to 40 km^2 (Fig. 5), at elevations ranging from 30 to 120 m. The sandy substrates of savannas on the left margin of the Amazon River (Fig. 5a) are bordered by Paleozoic sedimentary rocks, mainly sandstones, siltstones and shales¹⁰⁰, outcropping at northwest, as the substrates of savannas on the right margin of the Amazon River (Fig. 5b and c) occur over lateritic paleosols¹⁰⁰. The studied savanna and upland forest substrates in eastern Amazonia are composed of

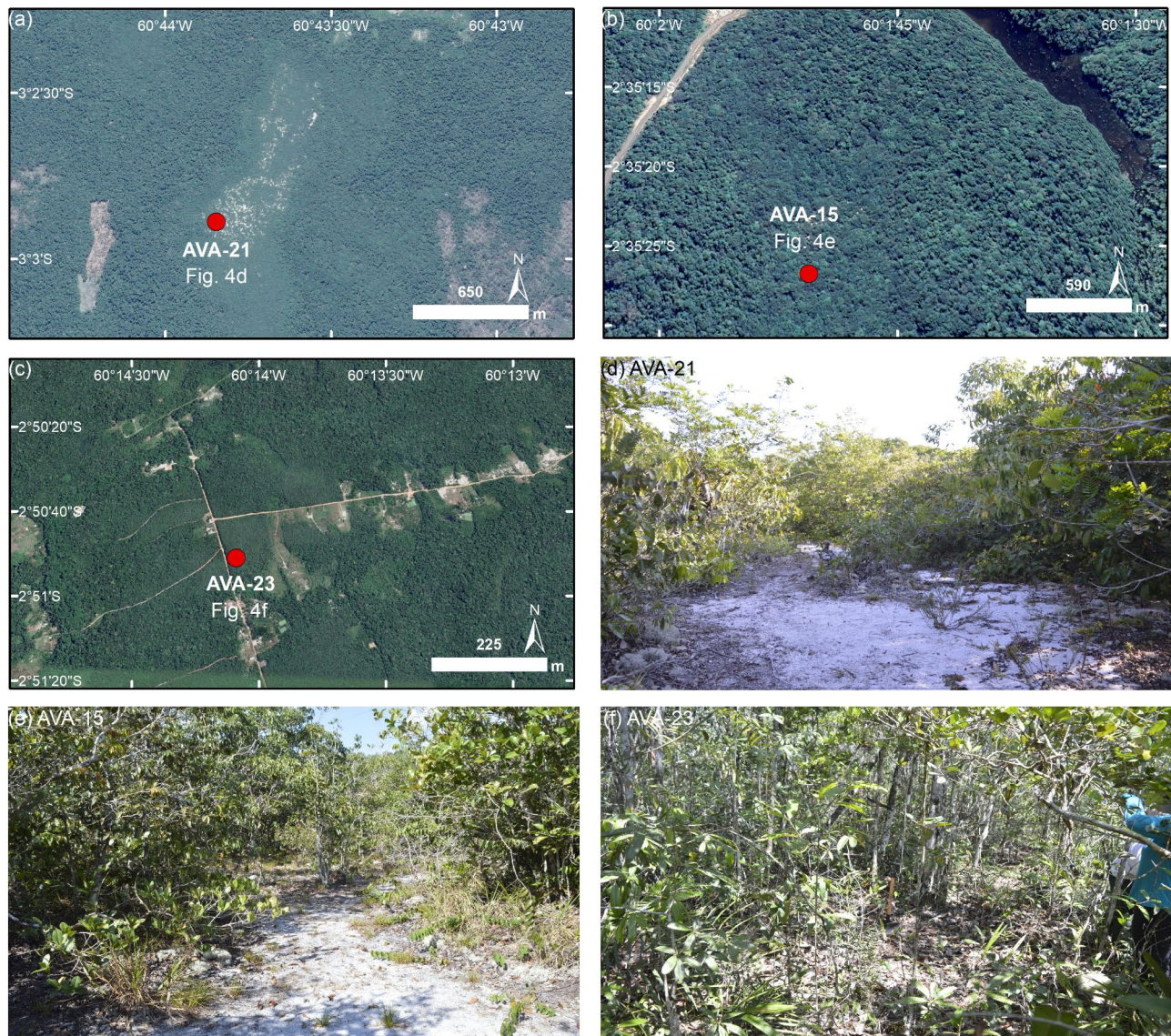


Fig. 4. Aerial (CNES/Airbus – Google Earth) and field views of WSE sampling sites AVA-21 (a,d), AVA-15 (b,e) and AVA-23 (c,f) in central Amazonia. Maps were created with ArcMap 10.8 software (<https://www.esri.com/en-us/arcgis/products/arcgis-desktop/resources>).

massive, loose, poorly to moderately selected light reddish, yellowish, and brownish medium sands, with the upper 10–20 cm of the deposits richer in organic matter and darker brown in color (Fig. 6c, d and e, and Figs. 7 and 8).

OSL ages

The majority of the studied sediment samples have quartz grains with rapidly decaying OSL signal, dominated by the fast component in the first 1 s of light emission and dose-response curves well described by linear (< 2 Gy) or single saturating exponential functions (5–50 Gy). Representative OSL decay curves with components deconvolution and dose-response curves are presented in SI1. The CAM D_e ranges from 0.7 ± 0.05 Gy to 52.3 ± 3.5 Gy, with approximately 60% of the samples having overdispersion $> 30\%$ (Table 3). MAM D_e ranges from 0.6 ± 0.04 Gy to 42.7 ± 0.01 Gy (Table 3). Samples have a wide range of thorium concentration (0.04–10.42 ppm), low uranium (0.23–1.10 ppm) and low ($< 0.02\%$) to undetectable potassium concentrations (Supplementary Table S1). Dose rate values vary from 0.24 to 1.08 Gy/ka, and with the WSE samples having lower dose rates (0.24–0.44 Gy/ka) than the savanna samples (0.40–1.08 Gy/ka) (Table 3, Supplementary Table S1). The cosmic dose rate contributes from 17 to 71% for the total dose rate, with an average of 35% (Supplementary Information SI1 and Table S1).

OSL ages in the substrate profiles of WSE in central Amazonia range from 4.2 ± 1.4 ka to 69.1 ± 5.9 ka for sediment samples retrieved until 2.1 m depth (Table 3; Fig. 7). The ages from savannas substrate profiles in eastern Amazonia range from 0.9 ± 0.1 ka to 65.1 ± 5.5 ka for sediment samples retrieved until 2.3 m depth

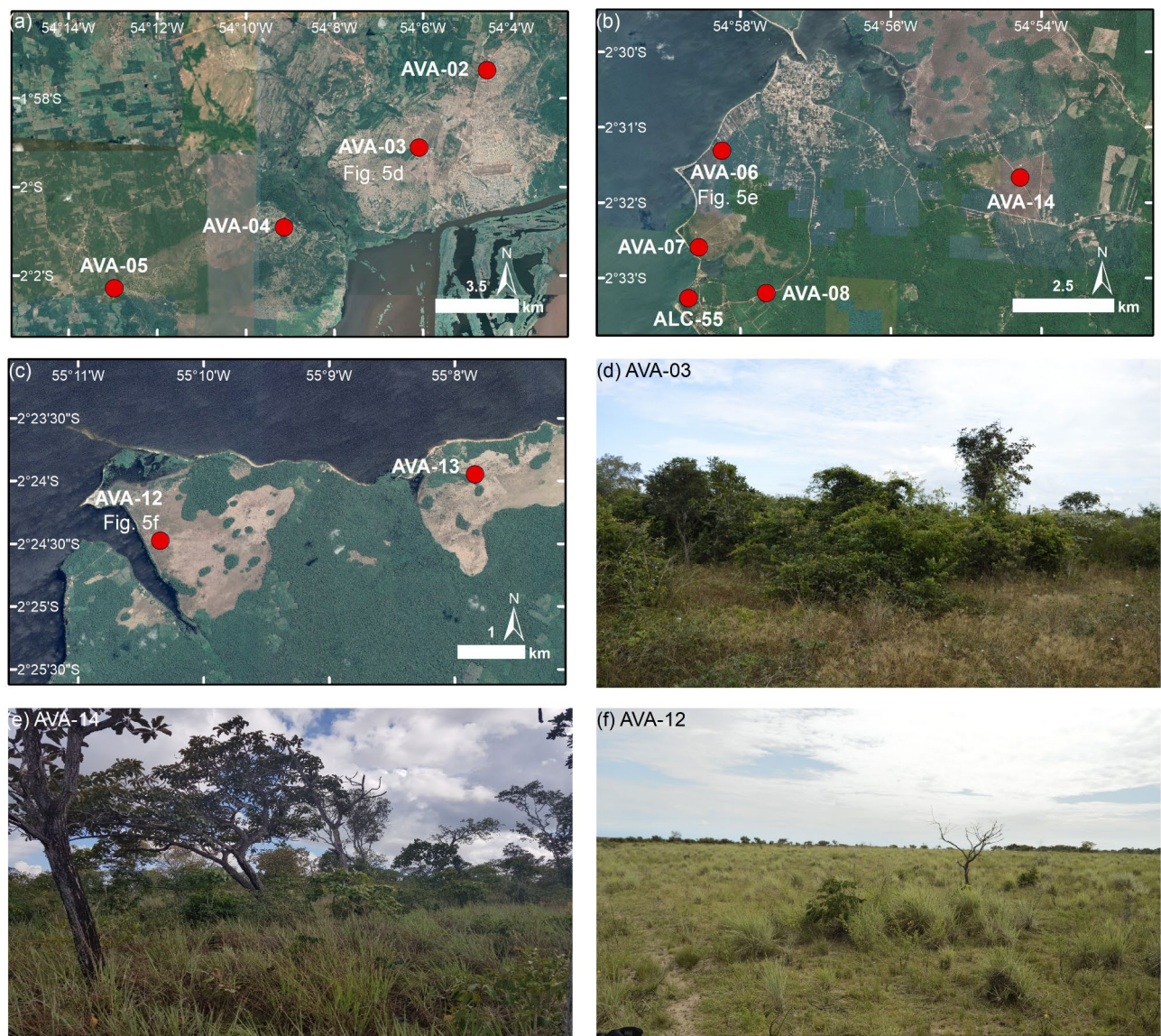


Fig. 5. Aerial (CNES/Airbus – Google Earth) views of savanna sampling sites AVA-02 to AVA-05 (a), AVA-06 to AVA-08, AVA-14 and ALC-55 (b) and AVA-12 and AVA-13 (c) in eastern Amazonia. Field views of savanna patches in sampling sites AVA-03 (d), AVA-14 (e) and AVA-12 (f). Maps were created with ArcMap 10.8 software (<https://www.esri.com/en-us/arcgis/products/arcgis-desktop/resources>).

(Table 3; Figs. 8 and 9). Both CAM and MAM ages point to a Holocene to Late Pleistocene age range (< 70 ka) for the studied sandy profiles (Figs. 7, 8 and 9).

OSL sensitivity

Average BOSL_{1s} sensitivity of pure quartz aliquots range in three orders of magnitude from 18 to 4234 cts Gy⁻¹ mg⁻¹ (Fig. 10a). The first second of light emission corresponds to 4 – 79% of the total 100 s light emission (Fig. 10b). Savanna substrate samples present higher average BOSL_{1s} (in both percentage and cts Gy⁻¹ mg⁻¹) than WSE samples, meaning that savanna substrate samples have brighter quartz grains. Samples of savanna substrates from eastern Amazonia have higher BOSL_{1s} sensitivity (~ 59–66% in average), similar to values reported for riverbed sediments of the Tapajós and Xingu rivers (43–57% in average) draining the Brazilian Shield in eastern Amazonia. WSE substrates have quartz with medium BOSL_{1s} sensitivity (~ 17–33% in average), which are more similar to values found in riverbed sediments of the Negro River (~ 14%) and higher than values of riverbed samples of the Amazon, Solimões and Madeira rivers (4–6%) (Fig. 10b).

Discussion

Origin of the sandy substrates supporting WSE and savannas in Amazonia

Combining OSL ages produced in this study with other luminescence ages previously published, the upper portion (< 3 m depth) of sandy substrates supporting WSE and savannas in northern, eastern and southern



Fig. 6. WSE substrates in sampling sites AVA-15 (a) and AVA-23 (b) in central Amazonia. Savanna substrates in sampling sites AVA-03 (c), AVA-06 (d) and AVA-12 (e) in eastern Amazonia. Upland forest substrate in sampling site AVA-08 (f) in eastern Amazonia.

Amazonia has ages between 120.6 and 0.7 ka, while the muddy substrates of the Beni savannas in southern Amazonia range from 37.4 to 2.9 ka (Fig. 11 and Supplementary Table S2). Published radiocarbon ages of substrates supporting different open vegetation ecosystems in Amazonia are mainly based on dating of bulk organic matter within the sediment, and the median ranges from 45.9 to 0.6 cal ka BP (Fig. 11 and Supplementary Table S2). Hence, substrates of current WSE and savannas across lowland Amazonia have ages restricted to the Late Pleistocene and Holocene, suggesting a marked synchronicity of substrate development in a ten-thousand-year timescale. However, accumulation rates of sandy substrates in WSE and savanna comprise three orders of magnitude, from $0.026 \text{ mm year}^{-1}$ to 1.3 mm year^{-1} (Fig. 12), pointing to significant differences in substrate aggradation in a local scale.

Quartz OSL ages can represent the last sediment deposition episode. In this case, OSL ages give an age estimate for sandy substrate formation and establishment of a specific patch of savanna or WSE. However, bioturbators in soil profiles can effectively transport grains to the surface, promoting OSL signal resetting through solar exposure followed by burial and OSL signal build up¹⁰¹, and increasing the overdispersion of D_e distributions toward a bias of underestimation of sediment deposition age. The AVA-02 profile comprises an upper sand layer deposited

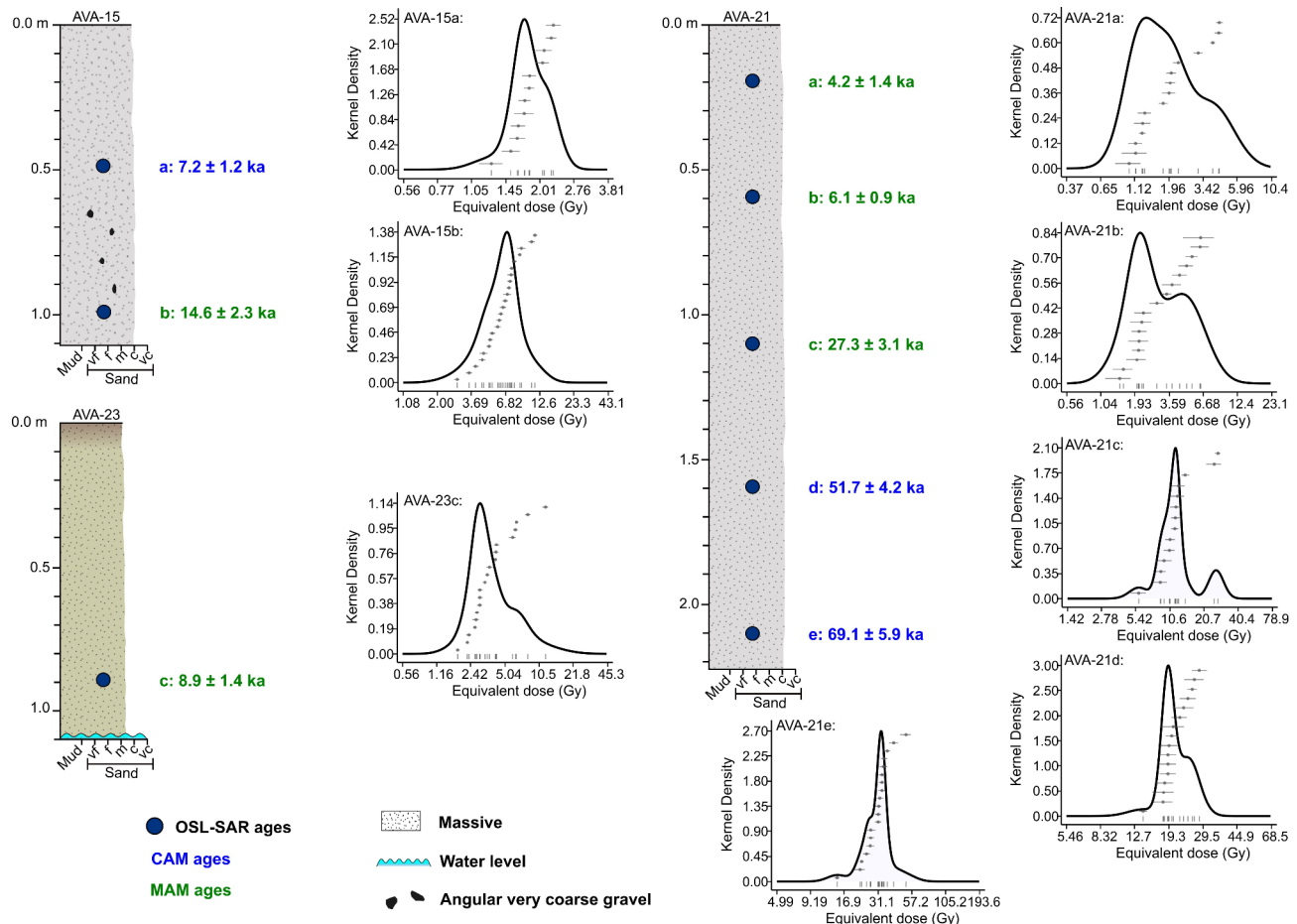


Fig. 7. Sedimentary profiles of WSE substrates in central Amazonia and their respective OSL ages and equivalent dose distribution.

from 2.7 to 2.1 ka, with an average aggradation rate of $1.29 \text{ mm year}^{-1}$, with low overdispersion (9–21%), which indicates a well bleached deposit almost undisturbed by soil mixing processes. Below 1.7 m, samples from profile AVA-02 (Fig. 8) have a D_e distribution with high dispersion (66–97%), suggesting a thorough mixing of grains after deposition, with MAM OSL ages of 17.8 to 4.4 ka. This suggests sediment deposition superimposed by autochthonous soil development. However, it is important to note that the D_e distribution is also a product of incomplete bleaching during sediment transport¹⁰², beta-dose heterogeneity¹⁰³, grain-to-grain luminescence behavior variability¹⁰⁴, and measurement and instrument uncertainties¹⁰⁵. The OSL ages presented in this study have D_e distribution with overdispersion within the range found in Amazonian fluvial or eolian deposits^{28,33}. They are also in the same range of radiocarbon ages obtained in correlative deposits. Thus, the OSL ages obtained in sandy substrates of WSE and savanna are interpreted as sediment deposition ages, despite some profiles can exhibit age underestimation.

Luminescence and radiocarbon ages provide a valuable temporal framework for the dynamics of WSE and savanna patches since approximately 120 ka, with a notable synchronicity and increase in substrate development within the last 23 ka across lowland Amazonia (Fig. 11). This pattern points to a regional control on the development of substrates supporting WSE and savannas. These ages are relatively younger than sediment deposition ages in fluvial terraces covered by upland rainforests in lowland Amazonia, which have sediment deposition ages older than around 45 ka²⁸. The younger ages of sandy substrates covered by WSE and savannas suggest increased sandy deposition on top of upland terraces since 23 ka, further increasing after the Last Glacial Maximum (LGM, 23–19 ka) (Fig. 11). This is synchronous with sediment accumulation within valleys of major Amazonian rivers, which fueled the regional expansion of floodplains after the LGM³⁶. The formation of massive sandy facies on top of upland terraces could be related with periods of increased surface water runoff leading to fast sand deposition by temporary streams flowing over upland terraces in areas with open canopy. The build and expansion of sandy substrates in upland terraces could favor the long-lasting establishment of open vegetation. However, massive sands can also be formed by soil processes and additional investigations are needed to elucidate the specific landscape and climate conditions responsible for accumulation of sands on top of upland fluvial terraces.

In Amazonia, quartz OSL sensitivity allows the discrimination of sediments transported by watersheds draining the Andes or cratonic areas⁴⁸. Thus, quartz OSL sensitivity can be used to interpret the provenance of

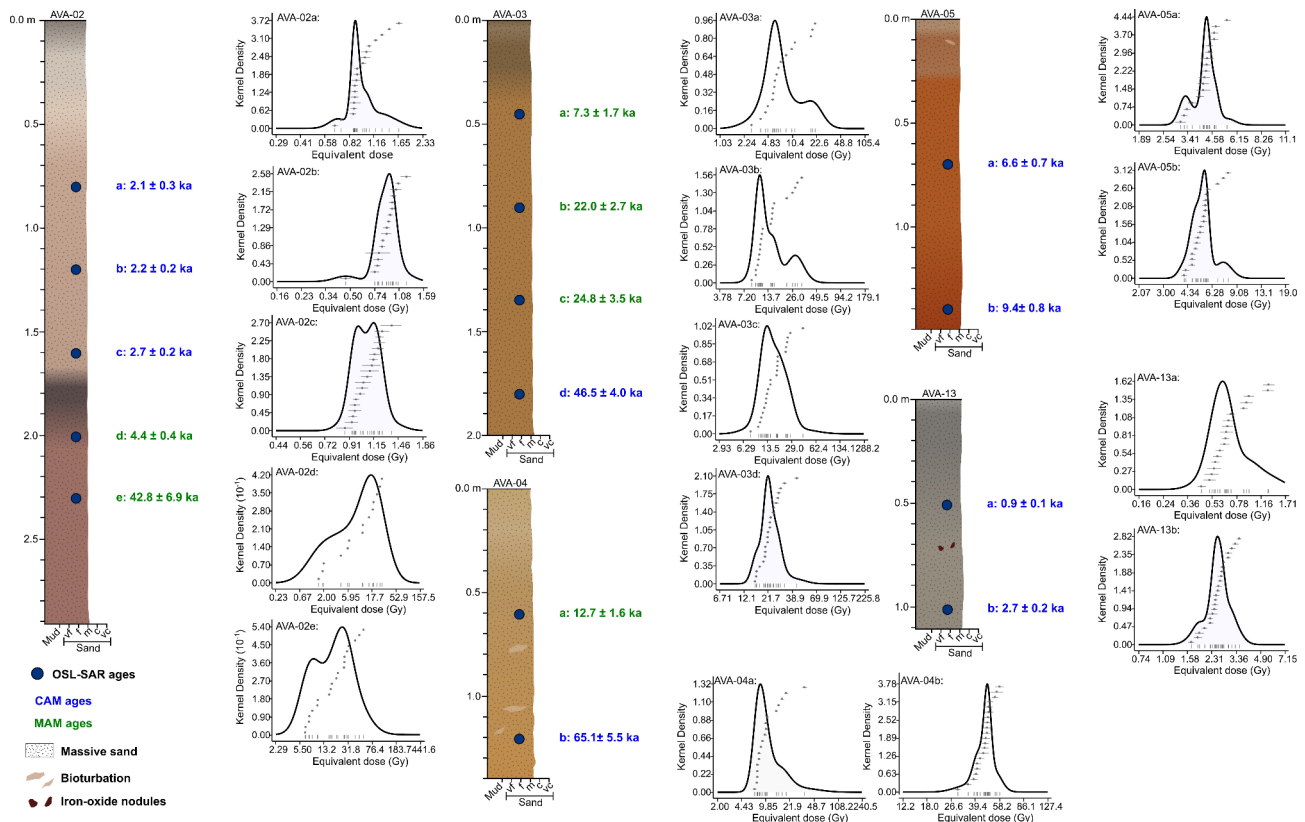


Fig. 8. Sedimentary profiles of savanna substrates in eastern Amazonia and their respective OSL ages and equivalent dose distribution.

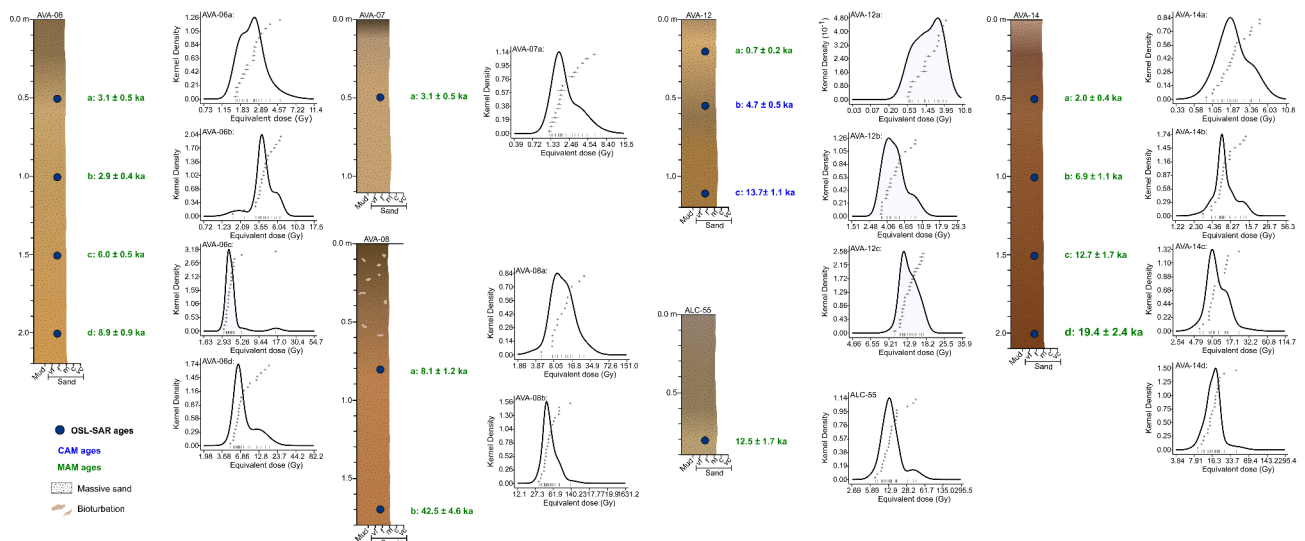


Fig. 9. Sedimentary profiles of savanna and upland forest (AVA-08) substrates in eastern Amazonia and their respective OSL ages and equivalent dose distribution.

Sample	Ecosystem	Depth (m)	Dose rate (Gy/ka)	Error (Gy/ka)	<i>n</i>	CAM (Gy)	Error (Gy)	OD (%)	MAM (Gy)	Error (Gy)	CAM Age (ka)	Error (ka)	MAM Age (ka)	Error (ka)
AVA-15a	WSE	0.50	0.25	0.04	12	1.8	0.1	13	2.0	0.1	7.2	1.2	7.9	1.3
AVA-15b	WSE	1.00	0.24	0.02	23	6.3	0.4	31	3.5	0.4	26.2	3.0	14.6	2.3
AVA-21a	WSE	0.20	0.30	0.10	15	2.0	0.3	48	1.3	0.1	6.7	2.4	4.2	1.4
AVA-21b	WSE	0.60	0.33	0.04	16	3.0	0.3	43	2.0	0.2	9.2	1.4	6.1	0.9
AVA-21c	WSE	1.10	0.37	0.03	14	12.0	1.2	37	10.0	0.9	32.7	4.0	27.3	3.1
AVA-21d	WSE	1.60	0.40	0.03	16	20.7	1.0	16	22.0	2.0	51.7	4.2	54.9	6.2
AVA-21e	WSE	2.10	0.44	0.03	19	30.1	1.7	24	19.2	3.3	69.1	5.9	44.1	8.2
AVA-23c	WSE	0.90	0.26	0.02	20	3.8	0.4	46	2.3	0.3	14.9	2.1	8.9	1.4
ALC-55	Savanna	0.80	0.70	0.07	24	14.6	1.3	42	8.8	0.9	20.8	2.7	12.5	1.7
AVA-02a	Savanna	0.80	0.46	0.05	19	1.0	0.1	21	0.859	0.002	2.1	0.3	1.8	0.2
AVA-02b	Savanna	1.20	0.40	0.04	17	0.88	0.04	18	0.83	0.01	2.2	0.2	2.1	0.2
AVA-02c	Savanna	1.60	0.40	0.03	19	1.07	0.03	9	1.06	0.05	2.7	0.2	2.6	0.2
AVA-02d	Savanna	2.00	0.42	0.03	14	8.6	2.2	97	1.8	0.1	20.2	5.4	4.4	0.4
AVA-02e	Savanna	2.30	0.42	0.03	20	18.0	2.7	66	7.5	0.6	42.8	6.9	17.8	1.8
AVA-03a	Savanna	0.45	0.46	0.09	18	7.4	1.0	56	3.4	0.4	16.1	3.8	7.3	1.7
AVA-03b	Savanna	0.90	0.48	0.05	20	14.6	1.3	36	10.6	0.7	30.4	4.1	22.0	2.7
AVA-03c	Savanna	1.35	0.44	0.04	23	16.4	1.3	38	10.9	1.3	37.3	4.3	24.8	3.5
AVA-03d	Savanna	1.80	0.49	0.04	23	22.7	1.1	23	18.7	1.6	46.5	4.0	38.3	4.3
AVA-04a	Savanna	0.60	0.64	0.07	18	10.6	1.0	42	8.1	0.4	16.6	2.5	12.7	1.6
AVA-04b	Savanna	1.20	0.69	0.05	21	45.0	1.5	14	42.7	0.1	65.1	5.5	61.7	4.8
AVA-05a	Savanna	0.70	0.63	0.07	17	4.2	0.1	14	4.3	0.4	6.6	0.7	6.9	0.9
AVA-05b	Savanna	1.40	0.58	0.04	20	5.4	0.2	16	5.8	0.5	9.4	0.8	10.1	1.1
AVA-06a	Savanna	0.50	0.59	0.08	18	2.5	0.2	30	1.8	0.1	4.2	0.7	3.1	0.5
AVA-06b	Savanna	1.00	0.67	0.06	21	4.0	0.3	31	2.0	0.2	6.0	0.7	2.9	0.4
AVA-06c	Savanna	1.50	0.62	0.05	22	4.0	0.3	33	3.7	0.1	6.5	0.7	6.0	0.5
AVA-06d	Savanna	2.00	0.68	0.05	23	7.7	0.6	36	6.0	0.4	11.3	1.2	8.9	0.9
AVA-07a	Savanna	0.50	0.56	0.08	18	2.2	0.2	41	1.755	0.003	3.9	0.7	3.1	0.5
AVA-08a	Forest	0.80	0.75	0.07	15	11.3	1.3	44	6.0	0.8	15.2	2.2	8.1	1.2
AVA-08b	Forest	1.70	0.96	0.07	23	52.3	3.5	32	40.9	3.2	54.3	5.4	42.5	4.6
AVA-12a	Savanna	0.20	0.94	0.20	16	1.6	0.3	67	0.65	0.06	1.7	0.5	0.7	0.2
AVA-12b	Savanna	0.55	1.08	0.10	20	5.0	0.3	30	4.03	0.25	4.7	0.5	3.7	0.4
AVA-12c	Savanna	1.10	0.97	0.07	22	13.3	0.4	14	12.6	0.0	13.7	1.1	12.9	1.0
AVA-13a	Savanna	0.50	0.78	0.09	18	0.70	0.05	28	0.6	0.0	0.9	0.1	0.7	0.1
AVA-13b	Savanna	1.00	0.92	0.06	23	2.5	0.1	17	3.1	0.0	2.7	0.2	3.4	0.2
AVA-14a	Savanna	0.50	0.51	0.08	21	2.0	0.2	47	1.0	0.1	3.9	0.7	2.0	0.4
AVA-14b	Savanna	1.00	0.57	0.05	21	6.6	0.5	36	3.9	0.5	11.6	1.3	6.9	1.1
AVA-14c	Savanna	1.50	0.56	0.04	19	10.5	0.8	33	7.0	0.8	18.9	2.0	12.7	1.7
AVA-14d	Savanna	2.00	0.57	0.04	22	17.0	1.2	32	10.9	1.1	30.04	2.98	19.4	2.4

Table 3. Summary of OSL ages produced in this study. Detailed information of dose rate is presented in supplementary Table S1. N is the number of aliquots, OD is overdispersion, CAM is Central Age Model and MAM is minimum age model.

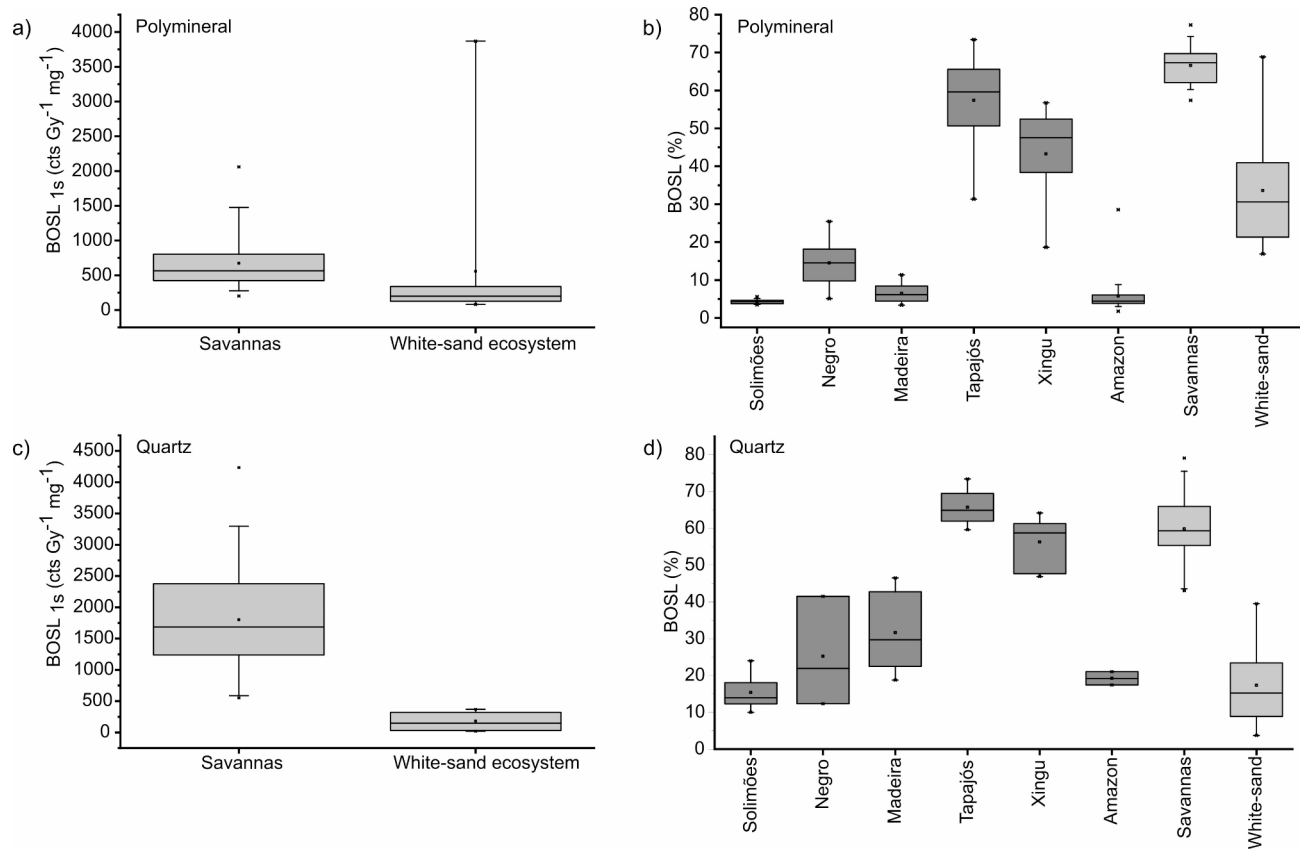


Fig. 10. BOSL_{1s} sensitivity as $\text{cts Gy}^{-1} \text{mg}^{-1}$ of quartz aliquots of the studied WSE and savanna substrates (a). % BOSL_{1s} sensitivity of pure quartz aliquots of the studied sandy substrates (on the right) and riverbed sands (b). Data from riverbed sands retrieved from Sawakuchi et al.⁴⁸.

sands forming substrates of the studied WSE and savanna. Quartz OSL sensitivity of savanna's substrate from eastern Amazonia is higher than quartz OSL sensitivity of WSE's substrate from central Amazonia (Fig. 10). This pattern matches with the OSL sensitivity of sediments transported by major rivers draining cratonic terrains of central and eastern Amazonia⁴⁸. The source of the eastern Amazonia savanna sandy substrate is similar to the present-day cratonic riverbed sediments of the Tapajós and Xingu Rivers, with headwaters in the *cerrado* (Brazilian savanna). Meanwhile, the source of the central Amazonia WSE substrate holds a higher similarity to the present-day riverbed sediments of the Negro River, a mixture of cratonic and Andean grains⁴⁸. This pattern indicates a link between sandy substrates of lowland open vegetation ecosystems and major rivers draining eastern and central Amazonia. This is in agreement with the hypothesis that the sandy substrates are formed by reworking (local erosion and deposition) of underlying fluvial deposits associated with the adjacent rivers.

Our results indicate that lowland open vegetation ecosystems can develop over substrates formed and degraded in a thousand-year timespan, such as sand accumulation on top of fluvial terraces during the Late Pleistocene and Holocene. Besides sand deposition by streams draining older fluvial deposits, channel avulsion in distributary fluvial systems can also favor the formation of wider sandy plains prone to establishment of open vegetation, such as in the Viruá megafan in northern Amazonia⁶⁷. The greater occurrence of WSE and savannas in the lowland portions of the Negro and Branco rivers basins (Fig. 1) can be explained by the sand-rich distributary fluvial systems occurring in these areas, forming extensive sandy alluvial plains, compared to contributary fluvial systems with muddy-dominated flooding plains prevailing along the Solimões-Amazon River in central and eastern Amazonia.

Fluvial systems in areas of northern Amazonia under the action of NE winds can also sustain the development of eolian dunes^{33,68,78}. Sand accumulation in eolian dunefields provides favorable edaphic conditions for the establishment of savanna vegetation. The higher elevation of dunefields hinders seasonal flooding and the high permeability of sands leads to deeper water table. Hence, in the Amazonian lowlands, higher availability of sandy substrates can be favored by the action of Quaternary fluvial, alluvial or eolian systems. Sandy substrates can also develop through in situ weathering of quartz-rich rocks in upland terrains. This is the main process responsible for sandy substrate development in highland areas, whose surface stability can reach million years timespans due to low denudation rates and lacking sediment accumulation¹⁰⁶. The uplift and weathering of ancient sandstones, such as the Late Cretaceous Alter do Chão Formation⁴⁴ in central and eastern Amazonia, promote the development of sandy substrates in highland areas over a million year timescale. The distribution of WSE in Amazonia (Fig. 1) is mostly contained within the region of shallow water table depth¹⁰⁷, and water-

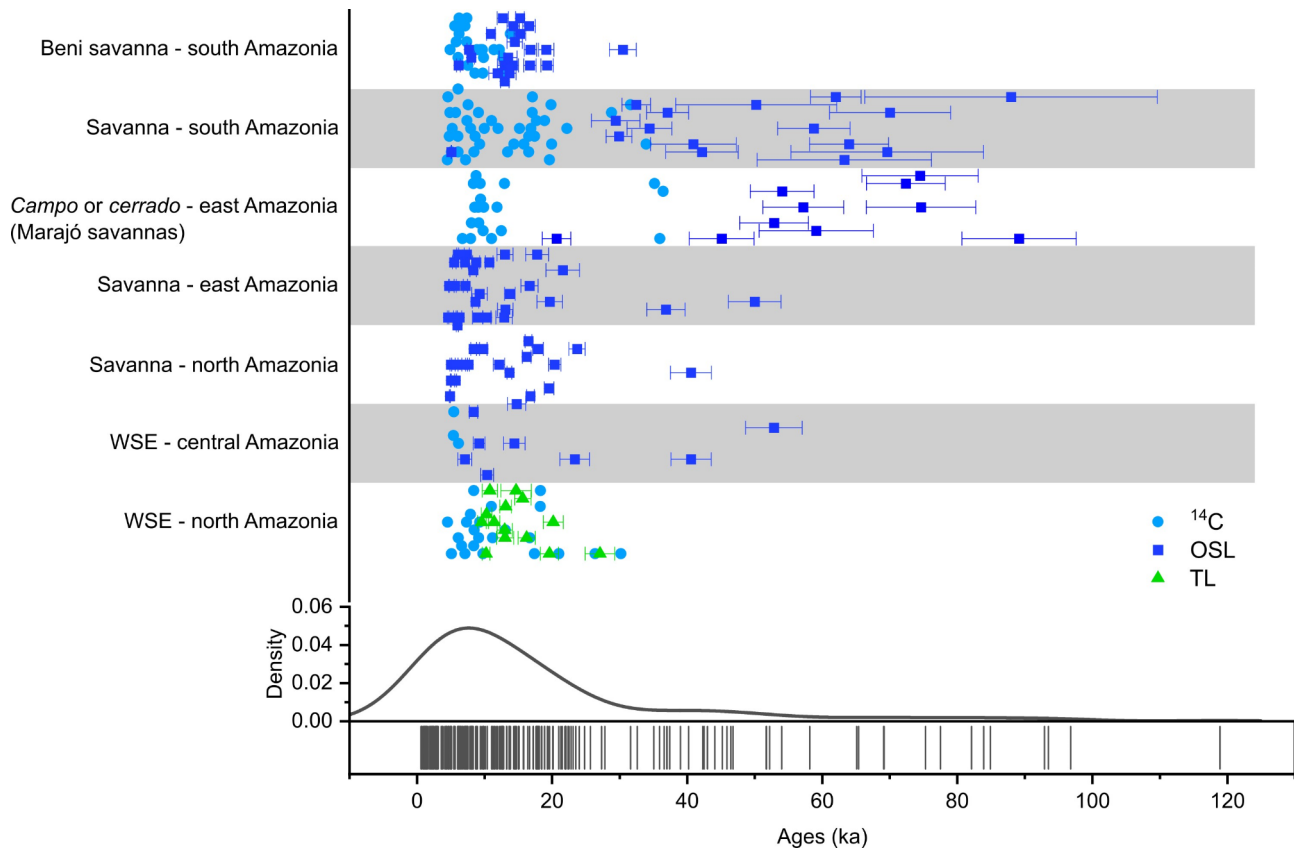


Fig. 11. Age compilation of substrate formation for different open vegetation ecosystems in Amazonia (full data for this compilation is in Supplementary Table S2) and density plot of the compiled ages. Y-axis is arbitrary for better visualization. C = radiocarbon dating, OSL = optically stimulated luminescence dating, TL = thermoluminescence dating.

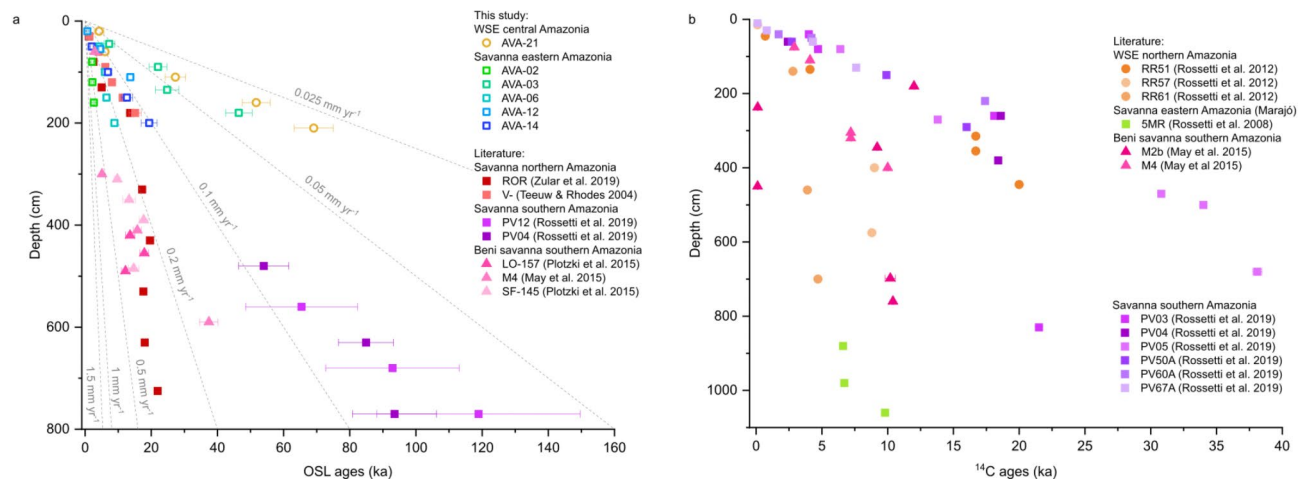


Fig. 12. (a) OSL age-depth compilation of substrate formation for WSE and savannas in Amazonia, dashed gray lines represent different accumulation rates of sandy substrates; (b) ^{14}C age-depth compilation of substrate formation for WSE and savannas in Amazonia. For these graphs, only profiles with 3 or more samples dated were considered.

table depth is an important control of WSE structure^{63,108}. This combination of local controls would explain the heterogeneous organization of WSE in relatively small patches, but frequent over the landscape.

Differently from the open-vegetation formations supported by sandy deposits, the Beni savannas in the Madeira River basin are established over more clayey and poorly drained substrates, formed by distributary

fluvial systems^{32,79}. These clayey substrates of the Beni savannas create an almost impermeable barrier that hinders water infiltration, leading to increased surface runoff. Unlike other Amazonian savannas, the Beni savannas experience both periods of seasonal flooding and extreme dryness^{82,109}. The seasonal flooding differs the Beni savanna from the upland savannas, whose main ecological constraint is an edaphic induced seasonal dryness due to marked water table fall favored by its sandy substrate.

The sandy terrains with different origins and development timespan ranging from thousand to million years can sustain a dynamic and long-term availability of substrates for colonization by open vegetation across Amazonia, with important implications for Amazonian biodiversity. The conditions needed to support the development of WSE and savannas in Amazonia depends on the occurrence of depositional or weathering sandy substrates combined with local hydrological variables, such as the amplitude of water table variation and drainage pattern (contributary or distributary), which in turn rely on climate and long-term drivers of topography. The local drivers lead to a partial decoupling between regional climate patterns and spatial distribution of open vegetation ecosystems.

Biotic implications of the landscape dynamics of open vegetation substrates

Plant and bird lineages exhibit high levels of species endemism in lowland WSE and have ages beyond the Quaternary^{2,60,110,111}, which does not fit the young sandy substrate ages reported here (Fig. 11). This indicates that these lineages have persisted in Amazonia for a long time, but their history has been dynamic during the Pleistocene, with spatiotemporal dynamism that follows the thousand-year dynamics of the substrate. Common population expansion for WSE specialist birds was detected in the Pleistocene at around 100 ka and 50 ka¹¹⁰, which may be related both to increasing availability of sandy substrates and consequently WSE patches, as shown here, and to changes in connectivity related to the strength of the closed canopy forest as a barrier for dispersion of these birds specialized in open vegetation. The period from 100 ka to 50 ka encompasses a major incision phase of lowland Amazonian rivers forced by falling sea level and increased precipitation phases³⁶, which increased the availability of upland terraces, including fluvial sandy facies, compared to seasonally flooded substrates. Forest permeability may also change in response to shifts in atmospheric CO₂ and precipitation patterns⁹, indicating that both regional climate and fluvial dynamics may have contributed to define the current distribution of biodiversity in WSE. WSE plants also occur on sandy soils formed through weathering of ancient Paleozoic to Mesozoic sandstones of the Solimões and Amazonas sedimentary basins and Proterozoic quartzites of the Guiana shield. These areas likely have more stable sandy substrates to host WSE plant populations over longer time periods beyond the Quaternary. Mesozoic and Paleozoic sandstones can also occur in lower elevation areas of central Amazonia (100–200 m), but their elevation is enough to hinder seasonal flooding and sediment accumulation by the Quaternary river system. This would predict that such higher elevation areas with soils over sand prone rocks harbor greater genetic variation and greater diversity than the more recent and dynamic WSE patches of lowland Amazonia under the influence of the Quaternary fluvial system.

In contrast to the Amazonian endemism of WSE taxa, taxa that occur in lowland Amazonian savannas are shared or have very recent connections with the biota of the large savannas surrounding Amazonia, including the savannas of Central Brazil and Guiana, the Chaco and the Llanos^{39,77,112}, which are not limited to sedimentary deposits and cover a variety of red soils. The occurrence of widespread areas of savanna surrounding Amazonia is largely explained by the high precipitation seasonality. These regions host animal and plant species able to colonize patches of savanna within closed Amazonian forests such as the studied area near the Tapajós River mouth^{41,112}. In this case, the biota of the Amazonian savannas relies on diversification processes occurring in non-Amazonian savannas, such as the *cerrado* and the Llanos, whose spatiotemporal dynamics depend on regional and long term changes in climate and topography.

In the Guiana shield highlands, low denudation rate (0.01 to 0.04 mm yr⁻¹)¹⁰⁶ allows stable surfaces, where quartz-rich Precambrian rocks give rise to very shallow soils and exposed bedrock supporting the development of the Pantepui and rupestrian savannas, which have plant diversity similar to WSE. Phylogenetic and phylogeographic studies are still scarce for the Pantepui. Endemic frogs have very old origins, dating to 40 Ma¹¹³, studied plant clades originated from 12 to 2.5 Ma^{60,114,115}, and bird and plant diversity most likely originated during the Pliocene, with subsequent population divergence taking place in the Pleistocene¹¹⁶. Connectivity among Pantepui populations is suggested to be related to climate change that could cause variation in the vegetation along the valleys^{117,118}. Floristic relations between Pantepui savannas and lowland WSE are high^{63,118–120} because of shared ecological conditions of acidity, oligotrophy and water-logging, that represent a strong ecological filter for lineages. The stability of substrates over ancient sandy rocks (sandstones and quartzites) out of sedimentation by lowland rivers points that highland open vegetation ecosystems such as the Pantepui may also have served as long-term sources of diversity for the more dynamic lowland open vegetation patches covering Quaternary fluvial terraces.

Superimposed to sediment deposition and weathering processes, precipitation changes may exert a particularly strong influence on edaphically controlled areas. For instance, during drier LGM/Heinrich stadial 1 condition (from 23 to 14.8 ka) in northern Amazonian savanna⁶, fluvial channel sands became available for eolian transport forming new dunefield areas colonized by open vegetation³³. The shrinking of rainforest areas in eastern Amazonia is also attributed to low atmospheric CO₂ and precipitation reduction during the LGM^{11,12,15,88}. Thus, precipitation changes can influence upland vegetation directly through moisture availability or indirectly, promoting sedimentation and shifts in substrates and edaphic conditions. Direct or indirect effects of the South American Monsoon altering vegetation cover also leads to changes in surface runoff in sandy depositional systems. This could explain the concentration of upland sandy substrates ages after 23 ka and also suggest a common and regional mechanism controlling the development of the sandy substrates during this period. However, the precise mechanisms driving this synchronous pattern are not yet clear and need further investigation.

Conclusions

Increased and synchronous sand accumulation within the last 23 ka across lowland Amazonia over upland terraces created highly permeable substrates with deeper water table, creating new areas colonized by WSE and savannas. Besides the formation of sandy substrates in a thousand-year timescale, weathering of ancient sandstones also favors the formation of sandy substrates in highland areas in a million-year timescale. The development of WSE and savannas in Amazonia relies on the deposition and weathering of sandy terrains, which leads to the occurrence of open vegetation patches within the upland rainforest even under the same regional climatic conditions. WSE and savanna biota predating the Quaternary period suggests a dynamic biotic history influenced by expansion and retraction of sandy substrates in lowland Amazonia. The formation of sandy substrates in time spans from thousands to millions of years, due to sand accumulation or weathering of older geological terrains, can maintain a dynamic and long-term supply of viable substrates for the colonization of upland open vegetation across lowland Amazonia. Thus, although open vegetation ecosystems have played an important role in the biogeographical history of Amazonia, glacial-interglacial cycles were probably not the main drivers of their distribution across Amazonia, as postulated in the refugia theory of biodiversification.

Data availability

All data generated or analysed during this study are included in this published article (and its supplementary information files). The datasets used and/or analyzed during the current study can also be made available from the corresponding author on reasonable request.

Received: 17 January 2024; Accepted: 10 September 2024

Published online: 01 October 2024

References

- Adeney, J. M., Christensen, N. L., Vicentini, A. & Cohn-Haft, M. White-sand ecosystems in Amazonia. *Biotropica* **48**, 7–23 (2016).
- Capururo, J. M. G. et al. Patterns and processes of diversification in amazonian white sand ecosystems: insights from birds and plants. *Neotropical Diversification: Patterns and Processes* (eds Rull, V. & Carnaval, A. C.) 245–270, Springer (2020).
- Haffer, J. Speciation in Amazonian forest birds. *Science* **165**, 131–137 (1969).
- Bush, M., Oliveira, P. E., Colinvaux, P., Miller, M. & Moreno, J. Amazonian paleoecological histories: one hill, three watersheds. *Palaeogeogr. Palaeoclimatol. Palaeoecol.* **214**, 359–393 (2004).
- Colinvaux, P. A., Oliveira, P. E. & Bush, M. B. Amazonian and neotropical plant communities on glacial time-scales: the failure of the aridity and refuge hypotheses. *Q. Sci. Rev.* **19**, 141–169 (2000).
- Häggi, C. et al. Response of the Amazon rainforest to late pleistocene climate variability. *Earth Planet. Sci. Lett.* **479**, 50–59 (2017).
- Kern, A. K. et al. A 1.8 million year history of Amazon vegetation. *Q. Sci. Rev.* **299**, 107867 (2023).
- Mayle, F. & Beerling, D. Late quaternary changes in amazonian ecosystems and their implications for global carbon cycling. *Palaeogeogr. Palaeoclimatol. Palaeoecol.* **214**, 11–25 (2004).
- Arruda, D. M., Schaefer, C. E. G. R., Fonseca, R. S. & Solar, R. R. C. Fernandes-Filho, E. I. Vegetation cover of Brazil in the last 21 ka: new insights into the amazonian refugia and pleistocene arc hypotheses. *Global Ecol. Biogeogr.* **27**, 47–56 (2018).
- D'Apolito, C., Absy, M. L. & Latrubesse, E. M. The Hill of six lakes revisited: new data and re-evaluation of a key Pleistocene Amazon site. *Q. Sci. Rev.* **76**, 140–155 (2013).
- Fontes, D. et al. Paleoenvironmental dynamics in South Amazonia, Brazil, during the last 35,000 years inferred from pollen and geochemical records of Lago do Saci. *Q. Sci. Rev.* **173**, 161–180 (2017).
- Mayle, F. E., Burbidge, R. & Killeen, T. J. Millennial-Scale Dynamics of Southern Amazonian Rain Forests. *Science* **290**, 2291–2294 (2000).
- Guimarães, J. T. F. et al. Lake sedimentary processes and vegetation changes over the last 45k cal a bp in the uplands of south-eastern Amazonia. *J. Quaternary Sci.* **36**, 255–272 (2021).
- Hermanowski, B., Costa, M. L., Carvalho, A. T., Behling, H. Palaeoenvironmental dynamics and underlying climatic changes in southeast Amazonia (Serra Sul Dos Carajás, Brazil) during the late Pleistocene and Holocene. *Palaeogeogr. Palaeoclimatol. Palaeoecol.* **365–366**, 227–246 (2012).
- Reis, L. S. et al. Hydroclimate and vegetation changes in southeastern Amazonia over the past ~25,000 years. *Q. Sci. Rev.* **284**, 107466 (2022).
- Reis, L. S. et al. Environmental and vegetation changes in southeastern Amazonia during the late Pleistocene and Holocene. *Quatern. Int.* **449**, 83–105 (2017).
- Hoorn, C., Lohmann, L. G., Boschman, L. M. & Condamine, F. L. Neogene History of the amazonian Flora: a perspective based on Geological, Palynological, and molecular phylogenetic data. *Annu. Rev. Earth Planet. Sci.* **51**, 419–446 (2023).
- Sato, H. et al. Dry corridors opened by fire and low CO₂ in amazonian rainforest during the last glacial Maximum. *Nat. Geosci.* **14**, 578–585 (2021).
- Silva, S. M. et al. A dynamic continental moisture gradient drove amazonian bird diversification. *Sci. Adv.* **5**, eaat5752 (2019).
- Wüster, W. et al. Tracing an invasion: landbridges, refugia, and the phylogeography of the neotropical rattlesnake (Serpentes: Viperidae: Crotalus durissus). *Mol. Ecol.* **14**, 1095–1108 (2005).
- Olson, D. M. et al. Terrestrial ecoregions of the World: A New Map of Life on Earth. *BioScience* **51**, 933–938 (2001).
- Projeto Radambrasil. Mosaicos semicontrolados de Radar. (1972).
- ter Steege, H. & Zondervan, G. A preliminary analysis of large-scale forest inventory data of the Guiana Shield. *Plant Diversity in Guyana: with Recommendations for a Protected Areas Strategy*, 35–54. Tropenbos Foundation, Wageningen, The Netherlands (2000).
- Vriesendorp, C. et al. Perú: Matsés. *Rapid Biological Inventories*. (2006).
- Josse, C. et al. Digital Ecological Systems Map of the Amazon Basin of Peru and Bolivia. (2007).
- Cremon, É. H., Rossetti, D. D. F., Sawakuchi, A. D. O. & Cohen, M. C. L. The role of tectonics and climate in the late quaternary evolution of a northern amazonian river. *Geomorphology* **271**, 22–39 (2016).
- Hayakawa, E. H. & Rossetti, D. F. Late quaternary dynamics in the Madeira river basin, southern Amazonia (Brazil), as revealed by paleomorphological analysis. *Acad. Bras. Ciénc.* **87**, 29–49 (2015).
- Pupim, F. N. et al. Chronology of Terra Firme formation in amazonian lowlands reveals a dynamic quaternary landscape. *Q. Sci. Rev.* **210**, 154–163 (2019).
- Rossetti, D. F., Toledo, P. M. & Góes, A. M. New geological framework for Western Amazonia (Brazil) and implications for biogeography and evolution. *Quat. res.* **63**, 78–89 (2005).

30. Rossetti, D. F., Vasconcelos, D. L., Valeriano, M. M. & Bezerra, F. H. R. Tectonics and drainage development in central Amazonia: the Juruá River. *CATENA* **206**, 105560 (2021).
31. May, J. H., Plotzki, A., Rodrigues, L., Preusser, F. & Veit, H. Holocene floodplain soils along the Río Mamoré, northern Bolivia, and their implications for understanding inundation and depositional patterns in seasonal wetland settings. *Sed. Geol.* **330**, 74–89 (2015).
32. Plotzki, A. et al. Geomorphology and evolution of the late pleistocene to Holocene fluvial system in the south-eastern Llanos De Moxos, Bolivian Amazon. *CATENA* **127**, 102–115 (2015).
33. Zular, A. et al. The role of abrupt climate change in the formation of an open vegetation enclave in northern Amazonia during the late Quaternary. *Glob. Planet Change* **172**, 140–149 (2019).
34. Prado, A. H., Almeida, R. P., Galeazzi, C. P., Sacek, V. & Schlunegger, F. Climate changes and the formation of fluvial terraces in central Amazonia inferred from landscape evolution modeling. *Earth Surf. Dynam.* **10**, 457–471 (2022).
35. Ribas, C. C., Aleixo, A., Nogueira, A. C. R., Miyaki, C. Y. & Cracraft, J. A palaeobiogeographic model for biotic diversification within Amazonia over the past three million years. *Proc. R. Soc. B* **279**, 681–689 (2012).
36. Sawakuchi, A. O. et al. Rainfall and sea level drove the expansion of seasonally flooded habitats and associated bird populations across Amazonia. *Nat. Commun.* **13**, 4945 (2022).
37. Oliveira-Filho, A. T. et al. On the floristic identity of Amazonian vegetation types. *Biotropica* **53**, 767–777 (2021).
38. Carvalho, W. D. & Mustin, K. The highly threatened and little known Amazonian savannahs. *Nat. Ecol. Evol.* **1**, 0100 (2017).
39. Resende-Moreira, L. C. et al. Evolving in isolation: genetic tests reject recent connections of Amazonian savannas with the central Cerrado. *J. Biogeogr.* **46**, 196–211 (2019).
40. Prance, G. T. Islands in Amazonia. *Philos. Trans. R. Soc. Lond. B.* **351**, 823–833 (1996).
41. Van Els, P. et al. Recent divergence and lack of shared phylogeographic history characterize the diversification of neotropical savanna birds. *J. Biogeogr.* **48**, 1124–1137 (2021).
42. Bezerra, I. S. A. A., Nogueira, A. C. R., Guimarães, J. T. F. & Truckenbrodt, W. Late pleistocene sea-level changes recorded in tidal and fluvial deposits from Itaúbal formation, onshore portion of the Foz do Amazonas Basin, Brazil. *Braz. J. Geol.* **45**, 63–78 (2015).
43. Rossetti, D. F. et al. The role of late pleistocene-holocene tectono-sedimentary history on the origin of patches of savanna vegetation in the middle Madeira River, southwest of the Amazonian lowlands. *Palaeogeogr. Palaeoclimatol. Palaeoecol.* **526**, 136–156 (2019).
44. Horbe, A. M. C., Horbe, M. A. & Suguio, K. Tropical spodosols in northeastern Amazonas State, Brazil. *Geoderma* **119**, 55–68 (2004).
45. Mafra, A. L., Miklós, A. A. W., Volkoff, B. & Melfi, A. J. Pedogênese numa seqüência latossolo-espodossolo na região do alto Rio Negro, Amazonas. *Rev. Bras. Ciênc. Solo* **26**, 381–394 (2002).
46. Sombroek, W. G. *Amazon Soils: A Reconnaissance of the Soils of the Brazilian Amazon Region*. Wageningen University and Research (1966).
47. Ribas, C. C., Fritz, S. C. & Baker, P. A. The challenges and potential of geogenomics for biogeography and conservation in Amazonia. *J. Biogeogr.* **49**, 1839–1847 (2022).
48. Sawakuchi, A. O. et al. Luminescence of quartz and feldspar fingerprints provenance and correlates with the source area denudation in the Amazon River basin. *Earth Planet. Sci. Lett.* **492**, 152–162 (2018).
49. Anderson, A. B. White-Sand Vegetation of Brazilian Amazonia. *Biotropica* **13**, 199 (1981).
50. Giulietti, A. M. et al. Edaphic Endemism in the Amazon: vascular plants of the canga of Carajás, Brazil. *Bot. Rev.* **85**, 357–383 (2019).
51. Hamilton, S. K., Sippel, S. J. & Melack, J. M. Seasonal inundation patterns in two large savanna floodplains of South America: the Llanos De Moxos (Bolivia) and the Llanos Del Orinoco (Venezuela and Colombia). *Hydrol. Process.* **18**, 2103–2116 (2004).
52. Huber, O. Neotropical savannas: Their flora and vegetation. *Trends Ecol. Evol.* **2**, 67–71 (1987).
53. Langstroth Plotkin, R. Biogeography of the Llanos De Moxos: natural and anthropogenic determinants. *Geogr. Helv.* **66**, 183–192 (2012).
54. Ratter, J. The Brazilian Cerrado Vegetation and threats to its Biodiversity. *Ann. Bot.* **80**, 223–230 (1997).
55. Sarmiento, G. *The Ecology of Neotropical Savannas*. (Harvard University, 1984).
56. Rull, V., Huber, O., Vegas-Vilarrubia, T. & Señaris, C. Definition and characterization of the Pantepui biogeographical province. *Biodiversity of Pantepui*. 3–32 (2019).
57. Briceño, H. O. & Schubert, C. Geomorphology of the Gran Sabana, Guayana Shield, southeastern Venezuela. *Geomorphology* **3**, 125–141 (1990).
58. Santos, J. O. S. et al. A New understanding of the provinces of the Amazon Craton based on integration of Field Mapping and U-Pb and Sm-Nd Geochronology. *Gondwana Res.* **3**, 453–488 (2000).
59. Voicu, G., Bardoux, M. & Stevenson, R. Lithostratigraphy, geochronology and gold metallogeny in the northern Guiana Shield, South America: A review. *Ore Geol. Rev.* **18**, 211–236 (2001).
60. Vicentini, A. The evolutionary history of *Pagamea* (Rubiaceae), a white-sand specialist lineage in Tropical South America. *Biotropica* **48**, 58–69 (2016).
61. Reatto, A. et al. Solos do bioma Cerrado: aspectos pedológicos. *Cerrado: Ecologia e Flora*. 109–149 (eds. Sano, S. M., Almeida, S. P. & Ribeiro, F. Planaltina, DF, Embrapa-CPAC, (2008).
62. Ribeiro, J. F. & Walter, B. M. T. As principais fitofisionomias do bioma Cerrado. *Cerrado: Ecologia e Flora*. 151–212 (eds. Sano, S. M., Almeida, S. P. & Ribeiro, F. Planaltina, DF, Embrapa-CPAC, (2008).
63. Vicentini, A. A vegetação ao longo de um gradiente edáfico no Parque Nacional do Jaú. *Janelas para a biodiversidade no Parque Nacional do Jaú: uma estratégia para o estudo da biodiversidade na Amazônia* 117–143 (eds Borges, S. H., Iwanaga, S., Durigan, C. C., & Pinheiro, M. R.) Manaus (2004).
64. Borges, S. H. et al. What is the avifauna of Amazonian white-sand vegetation? *Bird. Conserv. Int.* **26**, 192–204 (2016).
65. Roddaz, M., Viers, J., Brusset, S., Baby, P. & Héral, G. Sediment provenances and drainage evolution of the Neogene Amazonian foreland basin. *Earth Planet. Sci. Lett.* **239**, 57–78 (2005).
66. Roddaz, M., Baby, P., Brusset, S., Hermoza, W. & Maria Darrozes, J. Forebulge dynamics and environmental control in Western Amazonia: the case study of the Arch of Iquitos (Peru). *Tectonophysics* **399**, 87–108 (2005).
67. Rossetti, D. F., Zani, H., Cohen, M. C. L. & Cremon, É. H. A late pleistocene-holocene wetland megafan in the Brazilian Amazonia. *Sed. Geol.* **282**, 276–293 (2012).
68. Carneiro Filho, A., Schwartz, D., Tatumi, S. H. & Rosique, T. Amazonian paleodunes provide evidence for drier climate phases during the late Pleistocene-Holocene. *Quat. res.* **58**, 205–209 (2002).
69. Klinge, H. Podzol soils in the Amazon basin. *J. Soil Sci.* **16**, 95–103 (1965).
70. Duivenvoorden, J. F. & Lips, J. M. *A land-ecological Study of Soils, Vegetation, and Plant Diversity in Colombian Amazonia*. University of Amsterdam (1995).
71. Bleackley, D. & Khan, E. J. A. Observations on the white-sand areas of the Berbice Formation, British Guiana. *J. Soil Sci.* **14**, 44–51 (1963).
72. van Kekem, A. J., Pulles, J. H. M. & Khan, Z. *Soils of the Rainforest in Central Guyana*. (1996).
73. Bravard, S. & Righi, D. Geochemical differences in an oxisol-spodosol toposequence of Amazonia, Brazil. *Geoderma* **44**, 29–42 (1989).

74. Dubroeucq, D. & Volkoff, B. From Oxisols to Spodosols and histosols: Evolution of the soil mantles in the Rio Negro basin (Amazonia). *CATENA* **32**, 245–280 (1998).
75. Frasier, C. Amazonian lowland, white sand areas as ancestral regions for south American biodiversity: biogeographic and phylogenetic patterns in Potalia (Angiospermae: Gentianaceae). *Organisms Divers. Evol.* **8**, 44–57 (2008).
76. Heyligers, P. C. Vegetation and soil of a white-sand savanna in Suriname. *Mededelingen Van Het Botanisch Museum en Herbarium Van De Rijksuniversiteit Te Utrecht* **191**, 1–148 (1963).
77. Barbosa, R. I., Campos, C., Pinto, F. & Fearnside, P. M. *The Lavrados of Roraima*. Biodiversity and Conservation of Brazil's Amazonian Savannas (2007).
78. Teeuuw, R. M. & Rhodes, E. J. Aeolian activity in northern Amazonia: optical dating of late Pleistocene and Holocene palaeodunes. *J. Quaternary Sci.* **19**, 49–54 (2004).
79. Plotzki, A., May, J. H. & Veit, H. Review of past and recent fluvial dynamics in the Beni lowlands, NE Bolivia. *Geogr. Helv.* **66**, 164–172 (2012).
80. Suárez-Soruco, R. Compendio De geología de Bolivia. *Revista técnica De YPFB* **18**, (2000).
81. Plotzki, A., May, J. H., Preusser, F. & Veit, H. Geomorphological and sedimentary evidence for late Pleistocene to Holocene hydrological change along the Río Mamoré, Bolivian Amazon. *J. S. Am. Earth Sci.* **47**, 230–242 (2013).
82. Lombardo, U. Neotectonics, flooding patterns and landscape evolution in southern Amazonia. *Earth Surf. Dynam.* **2**, 493–511 (2014).
83. Rossetti, D. F., Valeriano, M. M., Góes, A. M. & Thales, M. Palaeodrainage on Marajó Island, northern Brazil, in relation to Holocene relative sea-level dynamics. *Holocene* **18**, 923–934 (2008).
84. Souza-Filho, P. W. M. et al. Mapping and quantification of ferruginous outcrop savannas in the Brazilian Amazon: A challenge for biodiversity conservation. *PLoS ONE* **14**, e0211095 (2019).
85. Bintanja, R. & Van De Wal, R. S. W. North American ice-sheet dynamics and the onset of 100,000-year glacial cycles. *Nature* **454**, 869–872 (2008).
86. Petit, J. R. et al. Climate and atmospheric history of the past 420,000 years from the Vostok ice core, Antarctica. *Nature* **399**, 429–436 (1999).
87. Govin, A. et al. Terrigenous input off northern South America driven by changes in Amazonian climate and the North Brazil Current retroflection during the last 250 ka. *Clim. Past* **10**, 843–862 (2014).
88. Wang, X. et al. Hydroclimate changes across the Amazon lowlands over the past 45,000 years. *Nature* **541**, 204–207 (2017).
89. Harris, I., Osborn, T. J., Jones, P. & Lister, D. Version 4 of the CRU TS monthly high-resolution gridded multivariate climate dataset. *Sci. Data.* **7**, 109 (2020).
90. Fick, S. E. & Hijmans, R. J. WorldClim 2: New 1-km spatial resolution climate surfaces for global land areas. *Intl J. Climatol.* **37**, 4302–4315 (2017).
91. Carvalho, L. M. V., Jones, C. & Liebmann, B. The South Atlantic Convergence Zone: Intensity, form, persistence, and relationships with Intraseasonal to Interannual Activity and Extreme Rainfall. *J. Clim.* **17**, 88–108 (2004).
92. Brugger, S. O. et al. Long-term man–environment interactions in the Bolivian Amazon: 8000 years of vegetation dynamics. *Q. Sci. Rev.* **132**, 114–128 (2016).
93. Carson, J. F. et al. Environmental impact of geometric earthwork construction in pre-columbian Amazonia. *Proc. Natl. Acad. Sci. U. S. A.* **111**, 10497–10502 (2014).
94. Murray, A. S. & Wintle, A. G. The single aliquot regenerative dose protocol: Potential for improvements in reliability. *Radiat. Meas.* **37**, 377–381 (2003).
95. Galbraith, R. F., Roberts, R. G., Laslett, G. M., Yoshida, H. & Olley, J. M. Optical dating of single and multiple grains of quartz from Jinmium rock shelter, northern Australia: Part I, experimental design and statistical models. *Archaeometry* **41**, 339–364 (1999).
96. Liang, P., Forman, S. L. & LDAC An Excel-based program for luminescence equivalent dose and burial age calculations. *Anc. TL* **37**, 21–40 (2019).
97. Guérin, G., Mercier, N. & Adamiec, G. *Dose-rate Convers. Factors: Update* **29**, (2011).
98. Prescott, J. R. & Hutton, J. T. Cosmic ray contributions to dose rates for luminescence and ESR dating: Large depths and long-term time variations. *Radiat. Meas.* **23**, 497–500 (1994).
99. Hogg, A. G. et al. SHCal20 Southern Hemisphere Calibration, 0–55,000 years cal BP. *Radiocarbon* **62**, 759–778 (2020).
100. CPRM. Geologia e Recursos Minerais Do Estado Do Pará. Escala 1:1.000.000. (2008).
101. Heimsath, A. M., Chappell, J., Spooner, N. A. & Questiaux, D. G. Creeping soil. *Geology* **30**, 111 (2002).
102. Singarayer, J. S., Bailey, R. M., Ward, S. & Stokes, S. Assessing the completeness of optical resetting of quartz OSL in the natural environment. *Radiat. Meas.* **40**, 13–25 (2005).
103. Olley, J. M., Roberts, R. G. & Murray, A. S. Disequilibria in the uranium decay series in sedimentary deposits at Allen's cave, nullarbor plain, Australia: Implications for dose rate determinations. *Radiat. Meas.* **27**, 433–443 (1997).
104. Adamiec, G. Variations in luminescence properties of single quartz grains and their consequences for equivalent dose estimation. *Radiat. Meas.* **32**, 427–432 (2000).
105. Thomsen, K. J., Murray, A. S. & Bøtter-Jensen, L. Sources of variability in OSL dose measurements using single grains of quartz. *Radiat. Meas.* **39**, 47–61 (2005).
106. Wittmann, H. et al. Sediment production and delivery in the Amazon River basin quantified by in situ-produced cosmogenic nuclides and recent river loads. *Geol. Soc. Am. Bull.* **123**, 934–950 (2011).
107. Targhetta, N., Kesselmeier, J. & Wittmann, F. Effects of the hydroedaphic gradient on tree species composition and aboveground wood biomass of oligotrophic forest ecosystems in the central Amazon basin. *Folia Geobot.* **50**, 185–205 (2015).
108. Damasco, G., Vicentini, A., Castilho, C. V., Pimentel, T. P. & Nascimento, H. E. M. Disentangling the role of edaphic variability, flooding regime and topography of a mazonian white-sand vegetation. *J. Veg. Sci.* **24**, 384–394 (2013).
109. Mayle, F. E., Langstroth, R. P., Fisher, R. A. & Meir, P. Long-term forest–savannah dynamics in the Bolivian Amazon: Implications for conservation. *Phil Trans. R. Soc. B.* **362**, 291–307 (2007).
110. Capurcho, J. M. G. et al. Phylogeographic and demographic patterns reveal congruent histories in seven amazonian White-Sand ecosystems birds. *J. Biogeogr.* **50**, 1221–1233 (2023).
111. Costa, F. M. et al. Islands in a green ocean: Spatially structured endemism in amazonian white-sand vegetation. *Biotropica* **52**, 34–45 (2020).
112. Devecchi, M. F. et al. Beyond forests in the Amazon: Biogeography and floristic relationships of the amazonian savannas. *Bot. J. Linn. Soc.* **193**, 478–503 (2020).
113. Kok, P. J. R. et al. Evolution in the south American 'Lost World': insights from multilocus phylogeography of stefanias (Anura, Hemiphractidae, *Stefania*). *J. Biogeogr.* **44**, 170–181 (2017).
114. Givnish, T., Millam, K., Berry, P. & Sytsma, K. Phylogeny, adaptive Radiation, and historical Biogeography of Bromeliaceae inferred from ndhF sequence data. *Aliso* **23**, 3–26 (2007).
115. Givnish, T. J. et al. Molecular evolution, adaptive radiation, and geographic diversification in the amphiatlantic family *Rapateaceae*: Evidence from NDHF sequences and morphology. *Evolution* **54**, 1915–1937 (2000).
116. Bonaccorso, E., & Guayasamin, J. M. On the origin of Pantepui montane biotas: a perspective based on the phylogeny of Aulacorhynchus toucans. *PLoS ONE* **8**(6), e67321 (2013).
117. Funk, V. A. & Brooks, D. R. *Phylogenetic Systematics as the Basis of Comparative Biology*. (1990).

118. Huber, O. Guayana highlands versus Guayana lowlands, a reappraisal. *Taxonomy* **37**, 595–614 (1988).
119. Berry, P. E. Floristic analysis and phytogeography. *Flora Venezuelan Guayana*. 161–191 (1995).
120. Steyermark, J. A. *Speciation and Endemism in the Flora of the Venezuelan Tepuis*. (1986).

Acknowledgements

We thank João P. S. de Cortes, Marina Maximiano and Julio I. B. Silva for their fieldwork assistance. We thank the Amazonian Biodiversity Studies Centre (CENBAM) and the National Institute for Amazonian Research (INPA) for their support during the fieldwork and permits for sampling in the Negro River Reserve for Sustainable Development (RDS Rio Negro). We also thank Thays Desiree, Luciana Nogueira and Ian del Río for their laboratory assistance. We sincerely thank the anonymous reviewers for their valuable feedback and constructive comments, which have significantly improved the quality of this manuscript.

Author contributions

FCGR, AOS and CCR contributed to the conception and design of the study. FCGR and AOS wrote the manuscript with the assistance of CCR, FNP, NP, TKA and AV. FCGR compiled OSL and radiocarbon age and carried out OSL measurements data analysis with the help of AOS, NP and FNP. FCGR, TKA and FNP participated in field surveys. CCR and AV contributed with interpretation of biotic implications. All authors contributed to manuscript revision, read, and approved the submitted version.

Funding

This research had the financial support of the Trans-Amazon Drilling Project (ICDP, US-NSF grants #EAR-1812857 and #EAR-1812681, FAPESP grant #2018/23899-2 and STRI), São Paulo Research Foundation (FAPESP grants #16/02656-9; #18/15123-4) and Conselho Nacional de Desenvolvimento Científico e Tecnológico (CNPq grant #062.01355/2018). FR is supported by FAPESP (grants #18/12472-8, 22/05520-1). AS and FP are supported by CNPq (grants #307179/2021-4; #302411/2018-6). TKA is supported by FAPESP (grants #2019/19948-0 and #2021/13129-8). Luminescence analyses were made in a laboratory created under the auspices of FAPESP (grant #09/53988-8).

Declarations

Competing interests

The authors declare no competing interests.

Additional information

Supplementary Information The online version contains supplementary material available at <https://doi.org/10.1038/s41598-024-72725-0>.

Correspondence and requests for materials should be addressed to F.C.G.R.

Reprints and permissions information is available at www.nature.com/reprints.

Publisher's note Springer Nature remains neutral with regard to jurisdictional claims in published maps and institutional affiliations.

Open Access This article is licensed under a Creative Commons Attribution-NonCommercial-NoDerivatives 4.0 International License, which permits any non-commercial use, sharing, distribution and reproduction in any medium or format, as long as you give appropriate credit to the original author(s) and the source, provide a link to the Creative Commons licence, and indicate if you modified the licensed material. You do not have permission under this licence to share adapted material derived from this article or parts of it. The images or other third party material in this article are included in the article's Creative Commons licence, unless indicated otherwise in a credit line to the material. If material is not included in the article's Creative Commons licence and your intended use is not permitted by statutory regulation or exceeds the permitted use, you will need to obtain permission directly from the copyright holder. To view a copy of this licence, visit <http://creativecommons.org/licenses/by-nc-nd/4.0/>.

© The Author(s) 2024